European Journal of Medicinal Chemistry 144 (2018) 612–625

Contents lists available at ScienceDirect

European Journal of Medicinal Chemistry

journal homepage: http://www.elsevier.com/locate/ejmech

Research paper

Structural and biological characterization of new hybrid drugs joining an HDAC inhibitor to different NO-donors

Sandra Atlante [a, 1], Konstantin Chegaev [b, 1], Chiara Cencioni [a, c], Stefano Guglielmo [b], Elisabetta Marini [b], Emily Borretto [b], Carlo Gaetano [a], Roberta Fruttero [b], Francesco Spallotta [a, *, 2], Loretta Lazzarato [b, **, 2]

[a] Division of Cardiovascular Epigenetics, Department of Cardiology, Goethe University, Frankfurt am Main 60596, Germany
[b] Dipartimento di Scienza e Tecnologia del Farmaco, Università degli Studi di Torino, 10125 Torino, Italy
[c] Istituto di Biologia Cellulare e Neurobiologia (IBCN), Consiglio Nazionale delle Ricerche (CNR), Roma, 00143, Italy

ARTICLE INFO

Article history:
Received 6 June 2017
Received in revised form
10 August 2017
Accepted 13 December 2017
Available online 15 December 2017

Keywords:
Histone deacetylases
Nitric oxide
Multitarget drugs
Muscle differentiation
Vasodilatation

ABSTRACT

HDAC inhibitors and NO donors have already revealed independently their broad therapeutic potential in pathologic contexts. Here we further investigated the power of their combination in a single hybrid molecule. Nitrooxy groups or substituted furoxan derivatives were joined to the α-position of the pyridine ring of the selective class I HDAC inhibitor MS-275. Biochemical analysis showed that the association with the dinitrooxy compound **31** or the furoxan derivative **16** gives hybrid compounds the ability to preserve the single moiety activities. The two new hybrid molecules were then tested in a muscle differentiation assay. The hybrid compound bearing the moiety **31** promoted the formation of large myotubes characterized by highly multinucleated fibers, possibly due to a stimulation of myoblast fusion, as implicated by the strong induction of myomaker expression. Thanks to their unique biological features, these compounds may represent new therapeutic tools for cardiovascular, neuromuscular and inflammatory diseases.

1. Introduction

Histone deacetylases (HDACs) are 18 enzymes grouped in four classes (HDAC I, II, III, IV), deputed to remove acetyl groups from lysine residues of histones and non-histone proteins. This epigenetic modification introduces positive charges in target proteins and prevents the introduction of other post-translation modifications (PTMs) including methylation, neddylation and ubiquitination [1]. In nucleosomes the presence of acetylated histones enables chromatin opening, DNA unwinding and consequent transcriptional activation. The removal of this PTM by HDACs leads to chromatin condensation and transcriptional silencing [2,3]. HDACs class I, II, IV are zinc-dependent metallo-proteins, whereas those belonging to class III, also named "sirtuins", are NAD^+-dependent enzymes. As HDACs induce structural changes into the chromatin that significantly alter cellular transcriptome, several pharmacologic tools have been generated so far to control their activity. Specifically, HDAC inhibitors (HDACi) have been developed for their ability to induce *in vitro* growth arrest, differentiation and/or apoptosis [4,5] as antitumor drugs [6]. In 2006, Vorinostat (suberoylanilide hydroxamic acid, SAHA), structurally similar to Trichostatin A (TSA), the first natural hydroxamic acid able to inhibit HDACs [7], has been approved by the food and drug administration (FDA) as HDAC inhibitor for the treatment of refractory cutaneous T-cell lymphoma [8]. Other more class-specific HDACi, are currently under phase II/III clinical trials as antitumor

* Corresponding author.
** Corresponding author.
E-mail addresses: sandra.atlas@yahoo.it (S. Atlante), konstantin.chegaev@unito.it (K. Chegaev), chcencioni@gmail.com (C. Cencioni), stefano.guglielmo@unito.it (S. Guglielmo), elisabetta.marini@unito.it (E. Marini), emily.borretto@gmail.com (E. Borretto), gaetano@em.uni-frankfurt.de (C. Gaetano), roberta.fruttero@unito.it (R. Fruttero), fspallotta@gmail.com (F. Spallotta), loretta.lazzarato@unito.it (L. Lazzarato).
[1] SA and KC contributed equally to this work.
[2] FS and LL jointly supervised this work.

https://doi.org/10.1016/j.ejmech.2017.12.047
0223-5234/

drugs [6,9]. The most recent drugs have been designed based on a pharmacophore model, where the crystal structure of the HDAC-like protein (HDLP), a homologue of mammalian class I/II HDACs, was complexed to SAHA and (*R*)- TSA [10,11]. This pharmacophore model, used to reveal the structure-activity relationships (SAR) of various inhibitor classes, contains a substructure able to bind the Zn^{2+} ion, present in the active site of the enzyme, a spacer, localized in the access channel to the active site, and a hydrophobic surface recognition group, which interacts with residues on the rim of the active site [12]. Very recent results show potential application of HDACi also in a number of non-cancer pathologies including inflammatory (eg. chronic obstructive pulmonary disease (COPD)), immunological (eg. asthma, rheumatoid arthritis) [13], neurological (eg, Alzheimer's and Parkinson's diseases), cardiovascular (eg. heart ischemia, heart failure, arrhythmia, cardiac hypertrophy) [14] and neuromuscular (eg. Duchenne and Becher's muscular dystrophies) [15–18] diseases. Specifically, class I HDACs are strongly activated and highly expressed in muscular dystrophies and their inactivation by HDACi or specific siRNAs is able to slow the disease progression [15–18]. Specifically, HDACi induce bigger myofiber size and counteract the continuous activation of satellite cells typical of dystrophic muscles by activation of the follostatin. The outcome of the HDACi treatment is resistance to muscle function degeneration and reduction of inflammatory infiltrate in dystrophic disease models and in humans [15,17,18]. Another physiopathological event associated with muscle dystrophies is the reduced nitric oxide (NO) availability, due to the altered relocation of the neuronal and endothelial NO synthase to the cytoplasm [19], leading to overproduction of oxygen and nitrogen reactive species. NO, an endogenous gaseous second messenger plays a pivotal role in a large number of physiopathological contexts. Its role in the vascular system is very well characterized: it contributes to maintain micro- and macro-vascular homeostasis inducing vasodilation, inhibition of platelet aggregation, modulation of leukocyte adherence to vessels and inhibition of smooth muscle cells proliferation [20,21]. NO is an important second messenger also in immunological and muscular systems. In the immune system, it works as one of the final effectors of the immune response triggering antimicrobial, antiparasitic and tumoricidal actions [22,23], being fundamental during the struggle against tumorigenesis and inflammation [24,25]. The anti-cancer action of NO is still under investigation: low doses may facilitate whereas high dosage seems counteracting cancer progression [20–23]. Indeed, high levels of NO exert cytostatic and/or cytotoxic effects on cancer cells by activation of pro-apoptotic signalling [26,27] and suppress metastasis by inhibition of epithelial-mesenchymal transition and reduction of invasive properties [28,29]. At the moment, NO donors are the only pharmacologic tools to reach the dosage necessary to exert both the anti-metastatic effect and the sensitization of cancer cells to chemotherapy and immunotherapy [30–33]. The high dose of NO necessary to achieve an anticancer effect, however, sets the limits for the use of these drugs in consequence of possible adverse systemic effects associated to pronounced vasodilation and toxic metabolites accumulation [34]. It is in this frame that the design of NO-hybrids could help to overcome clinical problems enhancing the specificity of NO action and minimizing its side effects. In skeletal muscles, NO modulates the contractile force of fast twitching fibres [35,36] and regulates regenerative processes of damaged muscles directly activating satellite cells, usually responsible of muscular regeneration [37–39]. NO donors showed beneficial effects in dystrophic muscles, thanks to their ability to slow down the disease progression [40–45]. In this context, the beneficial effect of NO donors has been also attributed to the property of NO to directly inhibit class I HDAC2 by both cysteine (S)-nitrosylation and tyrosine (Tyr)-nitration [3]. Indeed, dystrophic mice treated either with HDACi or NO donors showed overlapping rescuing features prompting us to develop a new class of hybrid drugs in which MS-275 (Entinostat; pyridin-3-ylmethyl 4-(2-aminophenylcarbamoyl) benzylcarbamate **1**), a selective class I HDAC inhibitor [46], was joined through an appropriate spacer to different NO-donor substructures, according to the scheme reported in Fig. 1. In our previous work [47] we already characterized the first example of this kind of hybrid compounds, here indicated as compound **2** (Fig. 1), which simultaneously released NO and regulated HDACs. In the present work we used as spacers either the methyl-aminomethyl- or the oxyethyloxy group, according to the synthetic pathway adopted. Either moieties bearing nitrooxy (ONO_2) groups or appropriately substituted furoxan (1,2,5-oxadiazole 2-oxide) derivatives were chosen as NO-donor substructures. It is generally accepted, in fact, that nitrooxy derivatives require enzymatic bioactivation to release NO, whereas furoxans require only thiol cofactors to do that [48,49]. Specifically, the NO-donor moiety was joined to the α-position of the pyridine ring present on the surface recognition region of MS-275. In this paper we report the synthesis, the structural characterization and the biochemical profile as HDAC inhibitors and as NO-donors of this new class of hybrid drugs.

2. Material and methods

2.1. Compound synthesis

^1H and ^{13}C NMR spectra were recorded on a Bruker Avance 300 at 300 and 75 MHz, respectively, using $SiMe_4$ as the internal standard, and the following abbreviations were used to indicate the peak multiplicity: s = singlet, d = doublet, t = triplet, qt = quartet, qi = quintet, m = multiplet, br s = broad signal. Low resolution mass spectra were recorded with a Finnigan-Mat TSQ-700 or with a Micromass Quattro micro TM API (Waters Corporation, Milford,

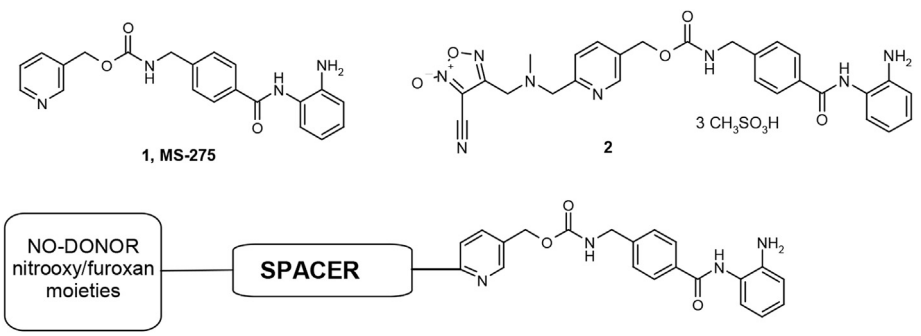

Fig. 1. Structure of MS-275 (1) and block structure of NO-donor MS-275 analogues.

MA, USA). Melting points were determined with a capillary apparatus (Buchi 540). Flash column chromatography was performed on silica gel (Merck Kieselgel 60, 230–400 mesh ASTM); PE stands for 40–60 petroleum ether. The progress of the reactions was followed by thin layer chromatography (TLC) on 5 cm × 20 cm plates with a layer thickness of 0.25 mm. Anhydrous sodium sulfate was used as the drying agent for the organic phases. Organic solvents were removed under vacuum at 30 °C. HPLC analyses were performed with a HP 1100 chromatograph system (Agilent Technologies, Palo Alto, CA, USA) equipped with a quaternary pump (model G1311A), a membrane degasser (G1379A), a diode-array detector (DAD) (model G1315B) integrated in the HP1100 system. Data analysis was done using a HP ChemStation system (Agilent Technologies). The analytical column was a Lichrospher C18 (4.6 × 250 mm, 5 μm) Merck. Preparative HPLC was performed on a Lichrospher C18 column (250 mm × 25 mm, 10 μm) (Merck Darmstadt, Germany) with a Varian ProStar mod-210 with Varian UV detector mod-325. High resolution mass spectra were recorded on a Bruker Bio Apex Fourier transform ion cyclotron resonance (FT-ICR) mass spectrometer equipped with an Apollo I ESI source, a 4.7 T superconducting magnet, and a cylindrical infinity cell (Bruker Daltonics, Billerica, MA, USA). Compounds **2** [47], **3** [50], **4** [51], **8** [52], **11** [53], **12** [53], **17** [47], **18** [54], **20** [55], 6-hydroxyhexane-1,2-diyl dinitrate [56] were synthesized according to literature.

2.1.1. 6-[2-(tert-Butyldimethylsilanyloxy)ethoxy]nicotinic acid methyl ester (5)

To a stirred solution of PPh_3 (4.1 g, 15.6 mmol) in dry 1,4-dioxane (60 mL) under positive nitrogen pressure, DIAD (3.2 mL, 16.2 mmol) was added dropwise at 0 °C. Stirring was continued for 15 min at room temperature (r.t.), then **3** (2.0 g, 13.1 mmol) was added. After 1 h stirring at r.t., **4** (2.3 g, 13.1 mmol) was added and the mixture was stirred overnight. The reaction mixture was concentrated under reduced pressure. The resulting brown oil was purified by flash chromatography (eluent PE/EtOAc 99/1 then 90/10 v/v) to give the title compound as a white solid (30% yield). M.p. 48.5–49.5 °C. ^{1}H-NMR (300 MHz, $CDCl_3$) δ = -0.08 (s, 6H, $(CH_3)_2Si$); 0.90 (s, 9H, $(CH_3)_3CSi$); 3.91 (s, 3H, $COOCH_3$); 3.97 (t, 2H, $SiOCH_2CH_2O$); 4.44 (t, 2H, $SiOCH_2CH_2O$); 6.78 (d, 1H, C_5H_3N); 8.14 (d, 1H, C_5H_3N); 8.80 (s, 1H, C_5H_3N). ^{13}C-NMR (75 MHz, $CDCl_3$) δ = -5.2; 18.4; 25.9; 52.0; 61.7; 67.8; 110.9; 119.6; 139.5; 150.0; 165.9; 166.5. MS CI $[M+H]^+$ *m/z* 312.

2.1.2. 6-[2-(tert-Butyldimethylsilanyloxy)ethyloxy]pyridin-3-ylmethanol (7)

To a suspension of $LiAlH_4$ (0.18 g, 4.80 mmol) in dry THF (30 mL), stirred under positive nitrogen pressure at −15 °C, a solution of **5** (2.99 g, 9.60 mmol) in dry THF (20 mL) was added dropwise. After 2 h, first H_2O (0.25 mL), second 15% NaOH (0.25 mL) and third H_2O (0.75 mL) were added. A rubbery white solid was filtered and washed with EtOAc (50 mL). The filtrate was washed with brine, dried, filtered and concentrated under reduced pressure. The yellow oil was purified by flash chromatography (eluent PE/EtOAc 80/20 v/v), to give the title compound as a pale yellow oil. (75% yield). ^{1}H-NMR (300 MHz, $CDCl_3$) δ = 0.08 (s, 6H, $(CH_3)_2Si$); 0.90 (s, 9H, $(CH_3)_3CSi$); 2.18 (br s, 1H, O*H*); 3.96 (t, 2H, $SiOCH_2CH_2O$); 4.36 (t, 2H, $SiOCH_2CH_2O$); 4.60 (s, 2H, CH_2OH); 6.75 (d, 1H, C_5H_3N); 7.59–7.63 (m, 1H, C_5H_3N); 8.06 (d, 1H, C_5H_3N). ^{13}C-NMR (75 MHz, $CDCl_3$) δ = −5.2; 18.4; 25.9; 61.9; 62.5, 67.3; 111.2; 129.0; 138.5; 145.6; 163.5. MS CI $[M+H]^+$ *m/z* 284.

2.2. General procedure for the preparation of Boc protected derivatives 9, 27–29

To a suspension of CDI (0.20 g, 1.1 eq) in dry THF (20 mL) under positive nitrogen pressure, the appropriate alcohol (1.10 mmol) was added dropwise. The mixture was stirred at r.t. for 3 h, then **8** (0.38 g, 1.10 mmol) was added. The mixture was stirred at r.t. overnight then was concentrated under reduced pressure and the residue was dissolved in CH_2Cl_2 (50 mL). The organic phase was washed twice with H_2O (30 mL) and brine (30 mL), dried, filtered and concentrated under reduced pressure. The crude products so obtained were purified by flash chromatography to give compounds **9**, **27**–**29** as white foams. Chromatographic eluents and yields of the products were as follow.

2.2.1. {2-[4-({6-[2-(tert-Butyldimethylsilanyloxy)ethoxy]pyridin-3-ylmethoxycarbonylamino}methyl)benzoylamino]phenyl}carbamic acid tert-butyl ester (9)

Eluent: CH_2Cl_2/MeOH 95/5 v/v; 70% yield.

^{1}H-NMR (300 MHz, $CDCl_3$) δ = 0.08 (s, 6H, $(CH_3)_2Si$); 0.90 (s, 9H, $(CH_3)_3CSi$); 1.50 (s, 9H, $(CH_3)_3CO$); 3.96 (t, 2H, $SiOCH_2CH_2O$); 4.36–4.43 (m, 4H, $SiOCH_2CH_2O$ + $C_6H_4CH_2$); 5.06 (s, 2H, $C_5H_3NCH_2$); 5.27 (br s, 1H, N*H*); 6.75 (d, 1H, C_5H_3N); 6.93 (s, 1H, C_6H_4); 7.12–7.35 (m, 5H, C_6H_4 + N*H*); 7.61 (d, 1H, C_6H_4); 7.76 (d, 1H, C_5H_3N); 7.90 (d, 2H, C_6H_4); 8.14 (s, 1H, C_5H_3N); 9.22 (br s, 1H, N*H*). ^{13}C-NMR (75 MHz, $CDCl_3$) δ = −5.2; 18.4; 25.9; 28.3; 44.7; 61.8; 64.3; 67.3; 81.4; 111.2; 124.5; 124.8; 125.8; 126.0; 127.5; 127.8; 130.0; 130.8; 133.4; 139.4; 142.5; 147.1; 154.7; 156.4; 163.9; 165.3. MS CI $[M+H]^+$ *m/z* 651.

2.2.2. (2-{4-[(6-{[Methyl-(3-nitrooxypropyl)amino]methyl}pyridin-3-ylmethoxycarbonylamino)methyl]benzoylamino}phenyl) carbamic acid tert-butyl ester (27)

Eluent: CH_2Cl_2/MeOH 98/2 v/v; 80% yield.

^{1}H-NMR (300 MHz, DMSO-d_6) δ = 1.45 (s, 9H, $(CH_3)_3CO$); 1.86 (qi, 2H, $CH_2CH_2CH_2$); 2.17 (s, 3H, CH_3); 2.45 (t, 2H, NCH_2); 3.60 (s, 2H, NCH_2Py); 4.30 (d, 2H, $NHCH_2$); 4.57 (t, 2H, CH_2ONO_2); 5.08 (s, 2H, CH_2O); 7.13–7.23 (m, 2H), 7.40–7.44 (m, 3H), 7.53–7.57 (m, 2H), 7.76 (d, 1H), 7.90–7.98 (m, 3H), 8.50 (s, 1H) (11 aromatic protons + 1H NH); 8.68 (s, 1H), 9.81 (s, 1H) (2H N*H*). ^{13}C-NMR (75 MHz, DMSO-d_6): δ = 23.9; 27.9; 41.8; 43.5; 52.7; 62.7; 63.1; 72.1; 79.6; 122.2; 123.8; 124.0; 125.5; 125.9; 126.9; 127.6; 129.7; 130.8; 131.6; 132.8; 136.1; 143.6; 148.2; 153.4; 156.2; 158.7; 165.0. MS ESI $[M+H]^+$ *m/z* 623.

2.2.3. (2-{4-[(6-{[(5,6-Bisnitrooxyhexyl)methylamino]methyl}pyridin-3-ylmethoxycarbonylamino)methyl]benzoylamino}phenyl) carbamic acid tert-butyl ester (28)

Eluent: CH_2Cl_2/MeOH 98/2 v/v; 40% yield.

^{1}H-NMR (300 MHz, DMSO-d_6) δ = 1.39–1.49 (m, 13H, $(CH_3)_3CO$ + 2 CH_2); 1.67–1.72 (m, 2H, CH_2) ($NCH_2CH_2CH_2CH_2$); 2.15 (s, 3H, CH_3); 2.37 (t, 2H, NCH_2); 3.59 (s, 2H, NCH_2Py); 4.29 (m, 2H, $NHCH_2$); 4.66–4.72 (m, 1H, $CH_aH_bONO_2$); 4.90–4.95 (m, 1H, $CH_aH_bONO_2$), 5.08 (s, 2H, CH_2O); 5.38–5.44 (m, 1H, $CHONO_2$); 7.15–7.20 (m, 2H), 7.39–7.45 (m, 3H), 7.52–7.56 (m, 2H), 7.74–7.77 (m, 1H), 7.89–7.95 (m, 3H), 8.49 (s, 1H) (11 aromatic protons + 1H N*H*); 8.67 (s, 1H, N*H*), 9.81 (s, 1H, N*H*). ^{13}C-NMR (75 MHz, $CDCl_3$): δ = 22.6; 26.6; 28.3; 29.3; 42.5; 44.6; 56.9; 63.4; 64.2; 71.3; 79.3; 81.1; 123.0; 124.5; 124.8; 125.5; 125.7; 126.0; 127.3; 127.8; 130.5; 133.2; 136.5; 137.1; 142.7; 148.7; 156.5; 158.8; 159.0; 165.7. MS ESI $[M+H]^+$ *m/z* 726.

2.2.4. (2-{4-[(6-{[(3-Carbamoylfuroxan-4-ylmethyl)methylamino]methyl}pyridin-3-yl- methoxycarbonylamino)methyl]benzoylamino}phenyl)carbamic acid tert-butyl ester (29)

Eluent: CH_2Cl_2/MeOH 95/5 v/v; 70% yield.

^{1}H-NMR ^{1}H-NMR (300 MHz, DMSO-d_6) δ = 1.45 (s, 9H, $(CH_3)_3CO$); 2.24 (s, 3H, CH_3); 3.79 (s, 2H, $NHCH_2Ph$); 3.96 (s, 2H); 4.30 (m, 2H) ($CH_2CH_3NCH_2$); 5.10 (s, 2H, CH_2O); 7.13–7.23 (m, 2H,

aromatic protons); 7.40–7.55 (m, 5H, aromatic protons); 7.77–7.98 (m, 4H, aromatic protons); 8.33 (br s, 1H, aromatic protons); 8.53 (br s, 2H, aromatic protons); 8.82 (br s, 1H, $CONH_2$); 9.82 (bs, 1H, $CONH_2$). ^{13}C-NMR (75 MHz, DMSO-d_6) δ = 27.9; 41.2; 43.5; 51.7; 61.8; 63.0; 66.7; 79.6; 110.7; 122.6; 123.8; 124.0; 125.5; 125.9; 126.9; 127.6; 129.7; 131.0; 132.8; 136.3; 143.6; 148.5; 153.4; 155.2; 155.7; 156.2; 157.5; 165.0. MS ESI [M+H]+ *m/z* 661.

2.2.5. [2-(4-{[6-(2-Hydroxyethoxy)pyridin-3-ylmethoxycarbonylamino]methyl}benzoylamino)phenyl]carbamic acid tert-butyl ester (10)

To a solution of **9** (0.35 g, 0.50 mmol) in distilled THF (10 mL), 1 M tetrabutylammonium fluoride in THF (0.78 mL, 0.70 mmol) was added. The solution was kept under stirring at r.t. for 3 h, then it was poured in H_2O and extracted with EtOAc (2 × 30 mL). The organic phases were washed with brine, dried, filtered and concentrated under reduced pressure. The yellow oil was purified by flash chromatography (eluent CH_2Cl_2/iPrOH 99/1 v/v), to give the title compound as a white foam (65% yield). ^{1}H-NMR (300 MHz, $CDCl_3$) δ = 1.49 (s, 9H, $(CH_3)_3CO$); 3.91 (m, 2H, $HOCH_2CH_2O$); 4.38–4.43 (m, 4H, $HOCH_2CH_2O$ + $C_6H_4CH_2$); 5.05 (s, 2H, $C_5H_3NCH_2$); 5.50 (br s, 1H, N*H*); 6.77 (d, 1H, C_5H_3N); 7.08–7.30 (m, 5H, C_6H_4 + N*H*); 7.62 (d, 1H, C_6H_4); 7.70 (d, 1H, C_5H_3N); 7.87 (d, 2H, C_6H_4); 8.09 (s, 1H, C_5H_3N); 9.28 (br s, 1H, N*H*). ^{13}C-NMR (75 MHz, $CDCl_3$) δ = 28.3; 44.6; 62.3; 64.1; 68.9; 81.2; 111.3; 124.5; 125.4; 125.7; 126.0; 127.3; 127.8; 130.3; 130.6; 133.3; 139.9; 142.5; 146.6; 154.6; 156.4; 163.8; 165.5. MS CI $[M+H]^+$ *m/z* 537.

2.3. General procedure for the preparation of BOC protected derivatives 13, 14

To a solution of **10** (0.40 g, 0.70 mmol) in CH_2Cl_2 or CH_3CN (5 mL), the appropriate furoxan derivative (0.70 mmol) and DBU (0.22 mL, 1.4 mmol) were added. The mixture was kept under stirring at r.t. for 18 h, then was poured in H_2O and extracted with CH_2Cl_2 (30 mL). The organic phase was washed with H_2O (2 × 20 mL) and brine, dried, filtered and concentrated under reduced pressure. The crude products so obtained were purified by flash chromatography to give compounds **13**, **14** as white foams. Chromatographic eluents and yields of the products were as follow.

2.3.1. {2-[4-({6-[2-(3-Phenylfuroxan-4-yloxy)ethoxy]pyridin-3-ylmethoxycarbonylamino}methyl)benzoylamino]phenyl}carbamic acid tert-butyl ester (13)

Eluent: CH_2Cl_2/MeOH 99/1 v/v; yield: 74% yield.

^{1}H-NMR (300 MHz, $CDCl_3$) δ = 1.51 (s, 9H, $(CH_3)_3CO$); 4.42–4.44 (m, 2H, FxOCH_2CH_2O); 4.83 (s, 4H, FxOCH_2CH_2O + $C_6H_4CH_2$); 5.08 (s, 2H, $C_5H_3NCH_2$); 5.17 (t, 1H, N*H*); 6.78–6.81 (m, 2H, C_5H_3N + aromatic protons); 7.14–7.23 (m, 4H, aromatic protons + N*H*); 7.36 (d, 2H, aromatic protons); 7.41–7.50 (m, 2H, aromatic protons); 7.64 (d, 1H, C_5H_3N); 7.80 (1d, H, aromatic protons); 7.92 (d, 2H, aromatic protons); 8.09–8.16 (m, 3H, aromatic protons + C_5H_3N); 9.18 (br s, 1H, N*H*). ^{13}C-NMR (75 MHz, $CDCl_3$): δ = 28.3; 44.7; 63.1; 64.2; 69.1; 81.4; 107.7; 111.1; 122.3; 124.5; 124.8; 125.6; 125.7; 126.0; 126.2; 127.1; 127.4; 127.8; 128.8; 129.9; 130.4; 130.8; 133.4; 139.7; 142.4; 147.0; 147.2; 154.6; 156.3, 162.2; 163.1; 165.2. MS ESI $[M+H]^+$ *m/z* 697.

2.3.2. {2-[4-({6-[2-(3-Phenylsulfonylfuroxan-4-yloxy)ethoxy] pyridin-3-ylmethoxycarbonylamino}methyl)benzoylamino]phenyl} carbamic acid tert-butyl ester (14)

Eluent: CH_2Cl_2/MeOH 99/1 v/v; yield: 70% yield.

^{1}H-NMR (300 MHz, $CDCl_3$) δ = 1.49 (s, 9H, $(CH_3)_3CO$); 4.40 (m, 2H, FxOCH_2CH_2O); 4.74 (br s, 4H, FxOCH_2CH_2O + $C_6H_4CH_2$); 5.08 (s, 2H, $C_5H_3NCH_2$); 5.49 (t, 1H, N*H*); 6.76 (d, 1H, C_5H_3N); 7.10–7.19 (m, 3H, aromatic protons); 7.27–7.32 (m, 3H, aromatic protons); 7.54 (t, 2H, aromatic protons); 7.64–7.73 (m, 3H, aromatic protons); 7.88 (d, 2H, aromatic protons); 8.01 (d, 2H, aromatic protons); 8.15 (br s, 1H, C_5H_3N); 9.35 (bs, 1H, N*H*). ^{13}C-NMR (75 MHz, $CDCl_3$): δ = 28.3; 44.7; 62.9; 64.4; 69.6; 81.3; 110.4; 111.0; 124.5; 125.7; 126.0; 127.4; 127.8; 128.5; 129.6; 130.2; 130.7; 131.7, 133.3, 135.6, 138.0; 139.7; 142.5; 147.0; 150.6; 154.6; 156.4; 158.8; 163.0; 165.4. MS ESI $[M+H]^+$ *m/z* 761.

2.3.3. 5,6-Bisnitrooxy-1-hexanmethansulfonate (19)

To a solution of 5,6-bisnitrooxy-1-hexanol (0.50 g, 2.20 mmol) in CH_2Cl_2 (20 mL), pyridine (0.36 mL, 4.40 mmol) was added. The mixture was stirred at 0 °C and methansulfonylchloride (0.51 mL; 6.60 mmol) was added dropwise. The mixture was stirred at r.t. for 6 h, then it was poured in H_2O and extracted with CH_2Cl_2 (3 × 20 mL). The organic phases were washed with 1 M HCl (30 mL) and brine, dried, filtered and concentrated under reduced pressure. The crude product was purified by flash chromatography (eluent PE/EtOAc 80/20 then 60/40 v/v), to give the title compound as a yellow oil (80% yield).

^{1}H-NMR (300 MHz, $CDCl_3$) δ = 1.54–1.71 (m, 2H), 1.78–1.88 (m, 4H) ($OCH_2CH_2CH_2CH_2$); 3.03 (s, 3H, CH_3); 4.26 (t, 2H, OCH_2CH_2); 4.47–4.53 (m, 1H, $CH_aH_bONO_2$), 4.75–4.80 (m, 1H, $CH_aH_bONO_2$); 5.27–5.34 (m, 1H, $CHONO_2$). ^{13}C-NMR (75 MHz, $CDCl_3$) δ = 21.1; 28.7; 37.4; 69.0; 71.1; 78.9. MS CI $[M+H]^+$ *m/z* 303.

2.4. General procedure for the preparation of alcohols 24–26

To a solution of **17** (0.88 g, 3.30 mmol) in acetone (10 mL), the appropriate NO-donor moiety (3.30 mmol) and $NaHCO_3$ (0.28 g, 3.30 mmol) were added. The mixture was stirred at the appropriate temperature until the completion of the reaction (6–24 h). The solvent was then evaporated under reduced pressure and the residue was dissolved in CH_2Cl_2 (50 mL). The organic phase was washed with water (2 × 30 mL) and brine, dried, filtered and concentrated under reduced pressure. Crude products (**21**–**23**) so obtained were partially purified by flash chromatography and use in the next synthetic step.

Appropriate *tert*-butyldimethylsilyl protected compound (1.1 mmol) was dissolved in CH_3COOH/H_2O/THF 3/1/1 v/v/v (15 mL). The mixture was kept under stirring at r.t. for 4 days. Then 2 M NaOH was added to reach pH 8. The mixture was extracted with CH_2Cl_2 (3 × 30 mL). The organic phases were washed with H_2O (2 × 30 mL), brine, dried and concentrated under reduced pressure. Crude products so obtained were purified by flash chromatography to give compounds **24**–**26** as oils. Chromatographic eluents and yields of the products were as follow.

2.4.1. (6-{[Methyl-(3-nitrooxy-propyl)amino]methyl}pyridin-3-yl) methanol (24)

First step. 24 h at r.t.; eluent: CH_2Cl_2/MeOH 99/1 v/v then 95/5 v/v; yield: 45%; pale yellow oil. **Second step**. Eluent CH_2Cl_2/MeOH 95/5 v/v; yield 80%; yellow oil.

^{1}H-NMR (300 MHz, $CDCl_3$) δ = 1.90 (qi, 2H, $CH_2CH_2CH_2$); 2.23 (s, 3H, CH_3); 2.50 (t, 2H, NCH_2); 3.61 (s, 2H, NCH_2Py); 4.51 (t, 2H, CH_2ONO_2); 4.67 (s, 3H, CH_2O + O*H*); 7.38 (d, 1H, C_5H_3N); 7.68–7.72 (m, 1H, C_5H_3N); 8.40 (m, 1H, C_5H_3N). ^{13}C-NMR (75 MHz, $CDCl_3$): δ = 24.6; 42.3; 53.1; 61.9; 63.3; 71.5; 123.0; 135.5; 135.7; 147.5; 157.8. MS CI $[M+H]^+$ *m/z* 256.

2.4.2. (6-{[(5,6-Bisnitrooxyhexyl)methylamino]methyl}pyridin-3-yl)methanol (25)

First step. 48 h at 50 °C; eluent: CH_2Cl_2 then CH_2Cl_2/MeOH 95/5 v/v; yield: 50%; yellow oil.

Second step. Eluent CH_2Cl_2/MeOH 95/5 v/v; yield: 65%; yellow

oil.

^{1}H-NMR (300 MHz, $CDCl_3$) δ = 1.41–1.62 (m, 4H), 1.68–1.79 (m, 2H) ($NCH_2CH_2CH_2CH_2$); 2.24 (s, 3H, CH_3); 2.44 (t, 2H, NCH_2); 3.63 (s, 2H, NCH_2Py); 4.36 (br s, 1H, OH); 4.43–4.50 (m, 1H, $CH_aH_bONO_2$); 4.70 (s, 2H, CH_2O); 4.72–4.77 (m, 1H, $CH_aH_bONO_2$), 5.24–5.32 (m, 1H, $CHONO_2$); 7.38 (d, 1H, C_5H_3N); 7.67–7.71 (m, 1H, C_5H_3N); 8.41 (m, 1H, C_5H_3N). ^{13}C-NMR (75 MHz, $CDCl_3$) δ = 22.6; 26.5; 29.0; 42.3; 56.8; 61.9; 63.2; 71.3; 79.3; 123.3; 135.5; 135.7; 147.6; 157.5. MS CI $[M+H]^+$ *m/z* 359.

2.4.3. 4-[(5-Hydroxymethylpyridin-2-ylmethyl)methylamino] methyl-3-furoxancarboxyamide (26)

First step. 6 h at r.t.; eluent: CH_2Cl_2/MeOH 99/1 v/v then 95/5 v/v; yield: 70%; pale yellow oil.

Second step. Eluent CH_2Cl_2/MeOH 99/1 v/v then 95/5 v/v; yield 80%; yellow oil.

^{1}H-NMR (300 MHz, $CDCl_3$) δ = 2.27 (s, 3H, CH_3); 3.81 (s, 2H, NCH_2Py); 3.98 (s, 2H, $FxCH_2N$); 4.56 (s, 2H, CH_2O); 5.35 (br s, 1H, OH); 7.41 (d, 1H, C_5H_3N); 7.74 (d, 1H, C_5H_3N); 8.36 (br s, 1H, $CONH_2$); 8.49 (s, 1H, C_5H_3N), 8.63 (br s, 1H, $CONH_2$). ^{13}C-NMR (75 MHz, $CDCl_3$): δ = 41.3, 51.8, 60.5, 62.0, 110.8, 122.6, 135.0, 136.1, 147.4, 155.3, 155.8, 156.2,. MS CI $[M+H]^+$ *m/z* 294.

2.5. General procedure for the preparation of chloride salts 15, 16, 30–32

To a solution of the appropriate Boc-protected derivatives (0.47 mmol) in dry 1,4-dioxane (4 mL), 5.30 M HCl solution in dry 1,4-dioxane (0.50 mL) was added. The mixture was kept under stirring at r.t. until the completion of the reaction (6–24 h). The solvent was removed and the obtained solid was triturated with dry CH_2Cl_2 until the formation of a white solid, which was filtered and dried to give compounds **15**, **16, 30**–**32**. Crude products so obtained were purified, if necessary, by preparative HPLC. Chromatographic eluents and yields of the products were as follow.

2.5.1. [4-(2-Aminophenylcarbamoyl)benzyl]carbamic acid 6-[2-(3-phenylfuroxan-4-yloxy)ethoxy] pyridin-3-ylmethyl ester dihydrochloride (15)

Crude product was purified by preparative HPLC (eluent CH_3CN/H_2O/HCl 60/40/0.05 v/v/v, flow = 20 mL/min, λ = 226 nm, injected 100 mg in 2 mL of CH_3CN/H_2O/DMSO 50/50/0.01). M.p. 113 °C (with decomposition). Yield: 68%.

^{1}H-NMR (300 MHz, DMSO-d_6) δ = 4.29 (d, 2H, $FxOCH_2CH_2O$); 4.79 (m, 4H, $FxOCH_2CH_2O + C_6H_4CH_2$); 5.02 (s, 2H, $C_5H_3NCH_2$); 6.91 (d, 1H, C_5H_3N); 7.34–7.65 (m, 10H, aromatic protons + NH_2); 7.77 (d, 1H, C_5H_3N); 7.94–7.99 (m, 3H, aromatic protons); 8.11 (d, 2H, aromatic protons); 8.21 (s, 1H, C_5H_3N); 10.61 (s, 1H, NH). ^{13}C-NMR (75 MHz, DMSO-d_6) δ = 43.6; 62.9; 63.2; 69.5; 107.6; 110.7; 121.9; 124.4; 126.0; 126.1; 126.3; 126.5, 126.8; 127.3; 128.2; 128.5; 129.0; 130.7; 132.0; 132.1; 140.2; 144.0; 146.7; 156.4; 162.2; 162.6; 165.5. MS ESI $[M+H]^+$ *m/z* 597.3. ESI-HRMS $[M+H]^+$: 597.2096, $C_{31}H_{29}N_6O_7$ requires 597.2092; HPLC purity >95%.

2.5.2. [4-(2-Aminophenylcarbamoyl)benzyl]carbamic acid 6-[2-(3-phenylsulfonylfuroxan-4-yloxy)ethoxy]pyridin-3-ylmethyl ester dihydrochloride (16)

Crude product was purified by preparative HPLC (eluent CH_3CN/H_2O/HCl 30/70/0.05 v/v/v, flow = 20 mL/min, λ = 226 nm, injected 100 mg in 2 mL of CH_3CN/H_2O/DMSO 50/50/0.01). M.p. 130 °C (with decomposition).Yield: 30%.

^{1}H-NMR (300 MHz, DMSO-d_6) δ = 4.27 (m, 2H, $FxOCH_2CH_2O$); 4.64–5.04 (m, 8H, $3CH_2 + NH_2$); 5.03 (s, 2H, $C_5H_3NCH_2$); 5.77 (s, 1H, NH); 6.60 (m, 1H, aromatic proton); 6.77–6.97 (m, 3H, aromatic protons); 7.16 (d, 1H, aromatic proton); 7.37 (d, 2H, aromatic protons); 7.66–7.95 (m, 9H, aromatic protons); 8.21 (s, 1H, NH); 9.63 (s, 1H, NH). ^{13}C-NMR (75 MHz, DMSO-d_6) δ = 43.6; 62.9; 63.1; 69.8; 110.5; 110.6; 116.1; 116.2; 123.3; 126.2; 126.7; 126.8; 127.8, 128.2; 130.0; 133.2; 136.1; 137.2; 140.1; 143.1; 146.8; 156.4; 158.8; 162.5; 165.1. MS ESI $[M+H]^+$ *m/z* 661.2. ESI-HRMS $[M+H]^+$: 661.1714, $C_{31}H_{29}N_6O_9S$ requires 661.1711.2092; HPLC purity >95%.

2.5.3. [4-(2-Aminophenylcarbamoyl)benzyl]carbamic acid 6-{[methyl-(3-nitrooxypropyl)amino]methyl}pyridin-3-ylmethyl ester trihydrochloride (30)

Pale yellow foam; yield: 80%.

^{1}H-NMR (300 MHz, DMSO-d_6) δ = 2.23 (qi, 2H, $CH_2CH_2CH_2$); 2.76 (s, 3H, CH_3); 3.22 (t, 2H, NCH_2CH_2); 4.30 (d, 2H, $NHCH_2$); 4.50 (s, 2H, NCH_2Py); 4.61 (t, 2H, CH_2ONO_2); 5.16 (s, 2H, CH_2O); 7.32–7.48 (m, 4H), 7.62–7.80 (m, 3H), 7.97 (d, 1H), 8.07–8.16 (m, 3H) (aromatic protons); 8.69 (s, 1H, NH), 10.63 (s, 1H, NH). ^{13}C-NMR (75 MHz, DMSO-d_6) δ = 21.3; 40.3; 43.6; 51.9; 58.1; 62.8; 70.8; 124.4; 125.5; 125.8; 126.3; 126.8; 127.3; 128.3; 128.4; 132.1; 132.2; 133.5; 137.4; 143.8; 148.4; 149.6; 156.2; 165.4. MS ESI $[M+H]^+$ *m/z* 523.3. ESI-HRMS $[M+H]^+$: 523.2304, $C_{26}H_{31}N_6O_6$ requires 523.2300; HPLC purity >95%.

2.5.4. [4-(2-Aminophenylcarbamoyl)benzyl]carbamic acid 6-{[(5,6-bisnitrooxyhexyl)methylamino]methyl}pyridin-3-ylmethyl ester trihydrochloride (31)

Pale yellow foam; yield: 68%.

^{1}H-NMR (300 MHz, DMSO-d_6) δ = 1.40 (qi, 2H, $CH_2CH_2CH_2$); 1.74 (m, 4H, $CH_2CH_2CH_2$); 2.74 (s, 3H, CH_3); 3.10 (m, 2H, CH_2) 4.31 (d, 2H, $NHCH_2$); 4.46 (s, 2H, NCH_2Py); 4.68–4.74 (m, 1H, $CH_aH_bONO_2$), 4.92–4.97 (m, 1H, $CH_aH_bONO_2$); 5.16 (s, 2H, CH_2O); 5.37–5.46 (m, 1H, $CHONO_2$); 7.32–7.54 (m, 5H), 7.53–7.70 (m, 2H), 7.91–7.95 (m, 1H), 8.04–8.11 (m, 3H); 8.68 (s, 1H, NH); 10.57 (s, 1H, NH); 10.92 (bs, 1H, exchangeable proton). ^{13}C-NMR (75 MHz, DMSO-d_6) δ = 21.4; 22.8; 27.7; 39.7; 43.6; 54.7; 58.0; 62.8; 71.8; 80.0; 124.3; 125.5; 125.8; 126.2; 126.7; 127.2; 128.2; 128.3; 132.0; 132.1; 133.4; 137.3; 143.8; 148.3; 149.7; 156.1; 165.3. MS ESI $[M+H]^+$ *m/z* 626. ESI-HRMS $[M+H]^+$: 626.2563, $C_{29}H_{36}N_7O_9$ requires 626.2569; HPLC purity >95%.

2.5.5. [4-(2-Aminophenylcarbamoyl)benzyl]carbamic acid 6-{[(3-carbamoylfuroxan-4-ylmethyl)methylamino]methyl}pyridin-3-ylmethyl ester trihydrochloride (32)

Crude product was purified by preparative HPLC (eluent CH_3CN/H_2O/HCl 60/40/0.05 v/v/v, flow = 20 mL/min, λ = 226 nm, injected 100 mg in 2 mL of CH_3CN/H_2O/DMSO 50/50/0.01). M.p. 102–106 °C (with decomposition).Yield: 52%.

^{1}H-NMR (300 MHz, DMSO-d_6) δ = 2.87 (s, 3H, CH_3); 4.30 (d, 2H, $NHCH_2Ph$); 4.65 (s, 2H), 4.78 (s, 2H) ($CH_2CH_3NCH_2$); 5.17 (s, 2H, CH_2O); 7.32–7.48 (m, 4H), 7.58–7.74 (m, 3H), 7.95–8.14 (m, 5H) (11 aromatic protons, 1H CONH); 8.79 (bs, 2H, 2CONH); 10.63 (s, 1H, CONH). ^{13}C-NMR (75 MHz, DMSO-d_6) δ = 41.0; 43.6; 49.6; 58.8; 62.7; 111.1; 124.4; 125.2; 125.8; 126.3; 126.8; 127.2; 128.3; 128.4; 132.2; 133.7; 138.0; 143.9; 147.8; 149.9; 151.3; 156.2; 156.3; 165.4. MS ESI $[M+H]^+$ *m/z* 561.3. ESI-HRMS $[M+H]^+$: 561.2208, $C_{27}H_{29}N_8O_6$ requires 561.2205; HPLC purity >95%.

2.5.6. 5,6-Bisnitrooxyhexyl-N,N-dmimethylamine oxalate (33)

To a solution of **19** (0.60 g, 2.00 mmol) in EtOH (15 mL) a solution 5.6 M of *N,N*-dimethylamine in MeOH (0.71 mL, 4.00 mmol) was added and the reaction mixture was heated at 50 °C for 24 h. The mixture was poured in water and 1 M NaOH was added (20 mL), then extracted with CH_2Cl_2 (2 × 15 mL), the organic phases were washed with brine, dried, filtered and concentrated under reduced pressure. The crude product was purified by flash chromatography (eluent CH_2Cl_2/MeOH 95/5 v/v). The resulting amine was dissolved

in EtOAc (15 mL), and a solution of oxalic acid (0.09 mg, 1.00 mmol) in EtOAc (5 mL) was added. The precipitate was filtered and washed with dry Et_2O to give the title compound as white solid. M.p. 95–96 °C. Yield: 49%.

^{1}H-NMR (300 MHz, DMSO-d_6) δ = 1.49 (m, 2H, $CH_2CH_2CH_2CH_2N$); 1.61–1.78 (m, 4H, $CH_2CH_2CH_2CH_2N$); 2.70 (s, 6H, $2CH_3$); 2.98 (t, 2H,$CH_2CH_2CH_2CH_2N$); 4.71 (dd, 1H, $CH_aH_bONO_2$); 4.93 (dd, 1H, $CH_aH_bONO_2$); 5.41 (m, 1H, $CHONO_2$). ^{13}C-NMR (75 MHz, DMSO-d_6) δ = 21.4; 23.3; 27.8; 42.1; 56.1; 71.9; 80.1; 164.7. MS ESI $[M+H]^+$ *m/z* 252. ESI-HRMS $[M+H]^+$: 252.1189, $C_8H_{18}N_3O_6$ requires 252.1190; HPLC purity >95%.

2.5.7. 3-Phenylsulfonyl-4-(2-methoxyethoxy)furoxan (34)

To a solution of 3,4-bisphenylsulfonylfuroxan (0.73 g, 2.00 mmol) in CH_2Cl_2 (30 mL) 2-methoxyethanol (0.24 mL, 3.00 mmol) and DBU (0.90 mL, 4.00 mmol) were added and the solution stirred at r.t. for 2 h. Then the reaction mixture was washed with H_2O (20 mL) and 1 M HCl (20 mL), dried, filtered and concentrated under reduced pressure. The crude product was purified by crystallization from iPr_2O to give the title compound as white solid. M.p. 111 °C. Yield: 52%.

^{1}H-NMR (300 MHz, DMSO-d_6) δ = 3.46 (s, 3H, OCH_3); 3.81 (t, 2H, CH_2OCH_3); 4.57 (t, 2H, $FxOCH_2CH_2$); 7.62 (m, 2H, C_6H_5); 7.76 (m, 1H, C_6H_5); 8.08 (m, 2H, C_6H_5). ^{13}C-NMR (75 MHz, DMSO-d_6) δ = 59.3; 69.7; 70.5; 110.0; 128.6; 139.6; 135.6; 138.1; 159.0. MS ESI $[M+Na]^+$ *m/z* 323. ESI-HRMS $[M+Na]^+$: 323.0310, $C_{11}H_{12}N_2NaO_6S$ requires 323.0308; HPLC purity >95%.

2.6. Vasodilating properties

Vasodilator activity was studied as previously described.[57] Briefly, thoracic aortas strips deprived of endothelium were isolated from male Wistar rats weighing 180–200 g. The tissues were mounted under 1.0 g tension in organ baths containing 30 mL of Krebs-bicarbonate buffer, maintained at 37 °C and continuously gassed with 95% O_2 − 5% CO_2 (pH = 7.4). After an equilibration period the aortic strips were contracted with L-phenylephrine (1 μM). When the response to the agonist reached a plateau, cumulative concentrations of the vasodilating agent were added. Effect of ODQ (1 μM) was evaluated in a separate series of experiments in which it was added to the organ bath 5 min before the contraction. Results were expressed as EC_{50} values; data are the mean ± SEM of at least three experiments. Responses were recorded by an isometric transducer connected to the MacLab System PowerLab. Addition of drug vehicle (1% DMSO) had not appreciable effect on contraction.

2.7. Cell culture

Transformed human keratinocytes (HaCaT) were grown at 37 °C in a 5% CO_2 atmosphere in complete Dulbecco's Modified Eagle Medium (DMEM, LONZA) supplemented with 1% (v/v) L-Glutamine (SIGMA), 1% (v/v) Penicillin-Streptomycin (SIGMA), 10% (v/v) Fetal Calf Serum (FCS, GIBCO). Cells were treated with the 2 hybrids at different concentrations (1, 10, 25, and 50 μM) for 1, 3 and 5 h to select the best concentration for biological evaluations. In all experiments, **1** and **33** or **34** were used as reference compounds and DMSO was used as solvent control.

2.8. Myoblast differentiation experiments

A cell line of murine myoblast (C2C12) was obtained by Cell Lines Service GmbH (CLS) and was cultured at 37 °C in a 5% CO_2 atmosphere in complete DMEM (SIGMA) containing 1% (v/v) L-Glutamine (LONZA), 1% (v/v) Penicillin-Streptomycin (SIGMA), 20% (v/v) Fetal Bovine Serum (FBS, Millipore). For differentiation experiments cells were kept in DMEM (SIGMA) with 2% Horse Serum (HS, SIGMA) for 5 days in presence or in absence of compounds **1**, **2**, **16**, **31**, **33**, **34** or **1** + **33**, **1** + **34** in combination. All compounds were used at 0.5 μM and renewed daily. Control cells were maintained in 20% serum (undifferentiated myoblast) or in the presence of vehicle (DMSO).

2.9. Cell cytotoxicity and viability

5×10^{-3} HaCaT or C2C12 cells were plated in each well of a 12-multiwell plate and treated for 72 h with vehicle alone (1% DMSO) or MS-275, **16**, **31** at different concentrations: a 0.1–100 μM range was used for HaCaT cells (1% DMSO final conc.) and a 0.5–10 μM range for C2C12 cells (1% DMSO final conc.). Cells were counted using Trypan Blue Stain (GIBCO) to discriminate alive from death cells. Results were expressed as percentage of dead cells (mean ± SEM) in comparison to total cell number. Three independent experiments were performed.

2.10. Nitric oxide production

Nitric oxide production was evaluated by adding 4,5-diaminofluorescein diacetate (DAF-2D) (Alexis), a sensitive fluorescent dye for detection of intracellular NO, to the complete medium 5 μM. At the end of treatment, cells were collected and analysed by fluorescence-activated cell sorting (FACS) to detect intracellular NO production. Upon entry into the cell, DAF-2D is transformed into the less cell-permeable DAF-2 by cellular esterases, thus preventing loss of signal due to diffusion of the molecule from the cell. In the presence of oxygen, DAF-2 reacts with NO to yield the highly fluorescent triazolofluorescein (DAF-2T).

2.11. HDAC assays

HDAC assays were performed with the HDAC colorimetric activity assay Kit (BioVision) according to manufacturer instructions. Briefly, HaCaT total cell lysates were obtained by mechanical lysis, using lysis buffer (10 mM Tris·HCl, pH 7.4, 150 mM NaCl, 1% NP-40, 1% sodium deoxycholate, 1% Triton x-100, 10% glycerol supplemented with 1 mM PMSF and protease inhibitor mix); 50 μg total extract were used in each experiment. Total extract was spotted directly onto a 96 multiwell plate provided in the kit, in the presence of HDAC assay buffer and HDAC substrate (acetylated lysine side chain). Control wells contained the same mixture plus TSA. Samples were assayed in duplicate. The mixture was incubated for 1 h at 37 °C; a lysine developer solution was then added and the plate was incubated for 30 min at room temperature (r.t.). The plate was read by colorimetric detection at wavelength 405 nm, using an ELISA reader (EnSpire Perkinelmer). Percent HDAC activity is shown with respect to the activity of HDAC alone (100%). The kit contains positive controls that consist of nuclear extract of HeLa. TrichostatinA (TSA) on HaCaT total cell lysate was used as a negative control.

To calculate IC50 values selectively on different HDAC isoforms HEK293T cells were transfected with 1 μg control plasmid (mock) or 1 μg plasmids expressing HDAC1, HDAC2 or HDAC3. Transfection was performed using Lipofectamine 3000 (Invitrogen) according the manufacturer's instruction. Plasmids: pCIG2/Flag-HDAC2 was a gift from Antonella Riccio, pcDNA3.1/Flag-HDAC1 (Addgene plasmid #13820) and pcDNA3.1/Flag-HDAC3 (Addgene plasmid #13819) were a gift from Eric Verdin [58]. Transfection was checked by Western blot and afterward cells were freshly lysed in RIPA buffer. 35 μg cellular extract was incubated with MS-275, **16** and **31** compounds at different concentration in the 0.1–100 μM range (1%

DMSO final conc.) or with solvent alone (1% DMSO) for 1 h at 37 °C and HDAC activity was measured as previously described. Selective HDAC isoform residual activity was determined by mock activity subtraction. Data are presented as means ± SE. Three independent experiments were performed.

2.12. Immunofluorescence analysis

Treated HaCaT cells were fixed in 4% paraformaldehyde solution and blocked for 1 h in PBS containing 10% bovine serum albumin (BSA). Cell fields were incubated with primary and secondary antibody in PBS containing 1% BSA. Nuclei were detected with Hoechst. Staining was visualized via an Apotome microscope; pictures were obtained using an Axiocam and analysed with KS 300 3.0 acquisition software (Zeiss). Myosin Heavy Chain staining: After 5 days of treatment, C2C12 cells were fixed and permealized in 4% paraformaldehyde. Fixed cells were blocked with 10% BSA/PBS, and incubated with MHC (anti-Myosin Heavy Chain (Millipore); diluted 1:50 in 1% BSA/PBS) and anti-mouse IgG-AlexaFluor-594 conjugated (Thermo Fisher Scientific). Cells were stained with DAPI to visualize cell nuclei. Images were captured on Axio Observer Z1 microscope (20× magnification) and analysed using digital image analysis software (AxioVision Rel. 4.8, Carl Zeiss).

2.13. Immunoprecipitation and western blotting

HDAC2 *S*-nitrosylation was determined by immunoprecipitation using anti-*S*-nitrosylation (SNOCys) (4 μg for 500 μg total proteins, polyclonal; Alpha Diagnostic) analysed by Western blotting with HDAC2 antibody (1:500, Santa Cruz). Immunoprecipitation experiments were performed using 500 μg total cell extract obtained by lysis in RIPA buffer (50 mM Tris·HCl (pH 7.4), 150 mM NaCl, 1% triton X100, 2 mM $MgCl_2$, and 1% sodium deoxycholate supplemented with 1 mM PMSF and protease/phosphatase inhibitor mix). Paramagnetic beads (Ademtech's Bioadembeads) were used for specific protein separation. Negative controls were run using the same amount of protein extract from WT samples immunoprecipitated with the corresponding purified IgG antisera (Santa Cruz) in the absence of primary antibody. HDAC overexpression was checked by Western Blotting with Flag antibody (1:2000, SIGMA) and GAPDH antibody (1:1000, Abcam).

2.14. RNA isolation and qRT-PCR

The analysis was performed on four independent experiments. Total RNA was extracted from C2C12 cells using Tri-Reagent (SIGMA) following supplier's instructions. The concentration and purity of the RNA samples were determined by Nanodrop1000. cDNA synthesis for quantitative real-time PCR (qRT-PCR) was carried out with SuperScript III First-Strand Synthesis Super Mix for qRT-PCR (Invitrogen) according to the manufacturer's protocol. All reactions were performed in 96-well format in the StepOne Plus Real-Time PCR System (Applied Biosystems) using PerfeCTa® SYBRGreen® FastMix®, ROX™ (Quanta BIOSCIENCES™). For each gene of interest, qRT-PCR was performed as follows: each RNA sample was tested in duplicate and P0 was used to normalize transcript abundance. mRNA expression levels were calculated by Comparative Ct Method by using the Applied Biosystem software (Applied Biosystem) and were presented as fold induction of transcripts for target genes. Fold change above 1 denotes upregulated expression, and fold change below 1 denotes downregulated expression versus the solvent.

List of forward and reverse primers:

Gene	Species	Forward (5′-3′)	Reverse (5′-3′)
Myomaker	*Mus Musculus*	ATCGCTACCAAGAGGCGTT	CACAGCACAGACAAACCAGG
Myogenin	*Mus Musculus*	GGGCAATGCACTGGAGTT	GACATATCCTCCACCGTGATG
MRF4	*Mus Musculus*	CAGCAAGAGAAGATGCAGGAG	CCTGGAATGATCCGAAACAC
P0	*Mus Musculus*	GCGTCCTGGCATTGTCTGT	GAAGGCCTTGACCTTTTCAGTAAG

2.15. Statistical analyses

Student's T test and ANOVA were used to assess statistically significant differences among different groups. A value of at least $P < .05$ was considered statistically significant.

3. Results and discussion

3.1. Chemistry: Synthesis

The synthetic strategy to obtain the final products **15**, **16** in which the oxyethyloxy group is present as linker is reported in Scheme 1. The 6-hydroxynicotinic acid methyl ester **3** was coupled in 1,4-dioxane solution with *tert*-butyldimethylsilyl-protected ethyleneglycol **4** in the presence of the adduct between Ph_3P and diisopropylazodicarboxylate (DIAD) (Mitsunobu conditions), to afford a mixture of compounds in which the O-alkylated **5** and the *N*-alkylated **6** products were present. After chromatographic separation, **5** was reduced with $LiAlH_4$ to the related alcohol **7**. Activation of **7** with *N*,*N*′-carbonyldiimidazole (CDI), followed by coupling in THF with [2-(4-aminomethylbenzoylamino)phenyl] carbamic acid *tert*-butyl ester (**8**) gave rise to the intermediate **9**. *tert*-Butyldimethylsilyl-protection was removed using tetrabutylammonium fluoride in THF to give the alcohol **10**. Nucleophilic displacement of the phenylsulfonyl-group in the furoxan derivatives **11** (3-phenyl-4-phenylsulfonylfuroxan) or **12** (3,4-bisphenylsulfonylfuroxan) gave rise to the *Boc*-protected final products **13**, **14** which, treated with 5.30 M HCl in 1,4-dioxane, produced the expected target compounds **15**, **16**.

The synthetic pathway to obtain the final products **30**–**32** in which the group methyl-aminomethyl- is present as linker is reported in Scheme 2. The *tert*-butyl (dimethyl)silyl-protected 5-(methylaminomethyl)pyridine-2-carbaldehyde **17** was prepared according to literature procedure [49]. Different NO-donor moieties were inserted on this scaffold using opportune alkylating agents: 3-bromopropylnitrate (**18**), 5,6-bisnitrooxyhexylmethanesulfonate (**19**), 4-bromomethylfuroxan-3-carboxamide (**20**) for the preparation of **21**–**23**, respectively. These products were deprotected with a mixture of $CH_3COOH/THF/H_2O$ (3/1/1 v/v/v) to afford the free alcohols **24**–**26**. Reaction of these intermediates with the *Boc*-protected amine **8** utilizing CDI in THF as activating reagent, gave rise to the *Boc*-protected products **27**–**29**, which, treated with 1,4-dioxane saturated with HCl, produced the expected target compounds**30**–**32**.

Compounds**33** and **34** were synthesized as reference

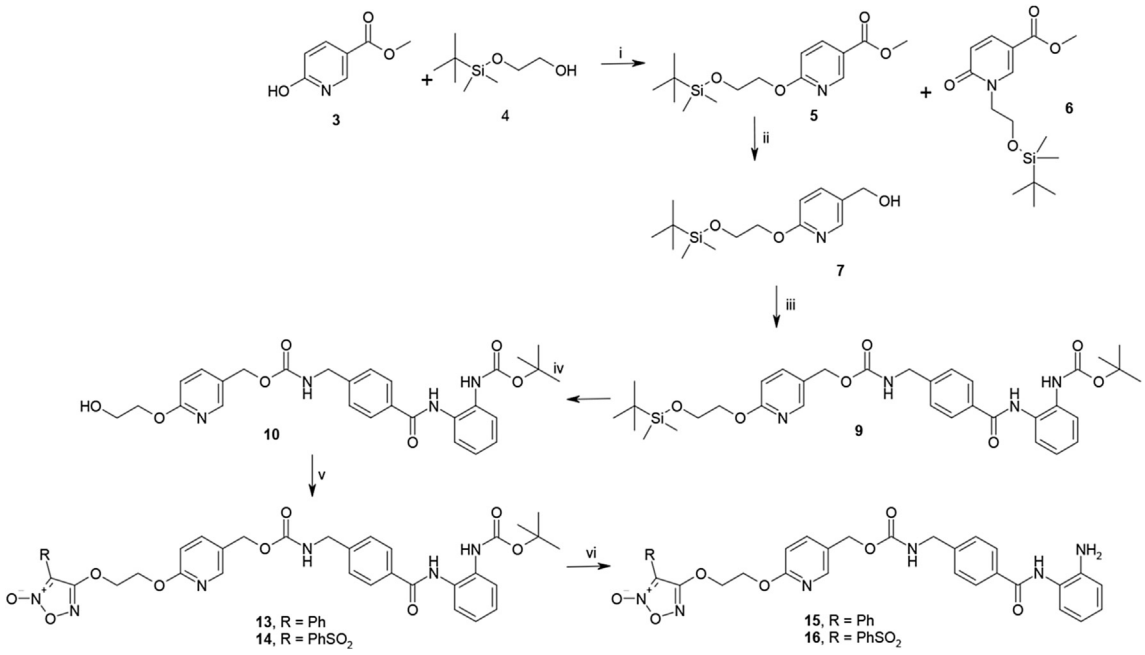

Scheme 1. Synthesis of compounds 15–16. Regents and conditions. i) Ph_3P, DIAD, 1,4-dioxane; ii) $LiAlH_4$, dry THF; iii) CDI, **8** ([2-(4-aminomethylbenzoylamino)phenyl]carbamic acid *tert*-butyl ester), dry THF; iv) TBAF, THF; v) **11** (3-phenyl-4-phenylsulfonylfuroxan), DBU, CH_3CN or **12** (3,4-bisphenylsulfonylfuroxan), DBU, CH_2Cl_2; vi) 5.30 M HCl in 1,4-dioxane, THF.

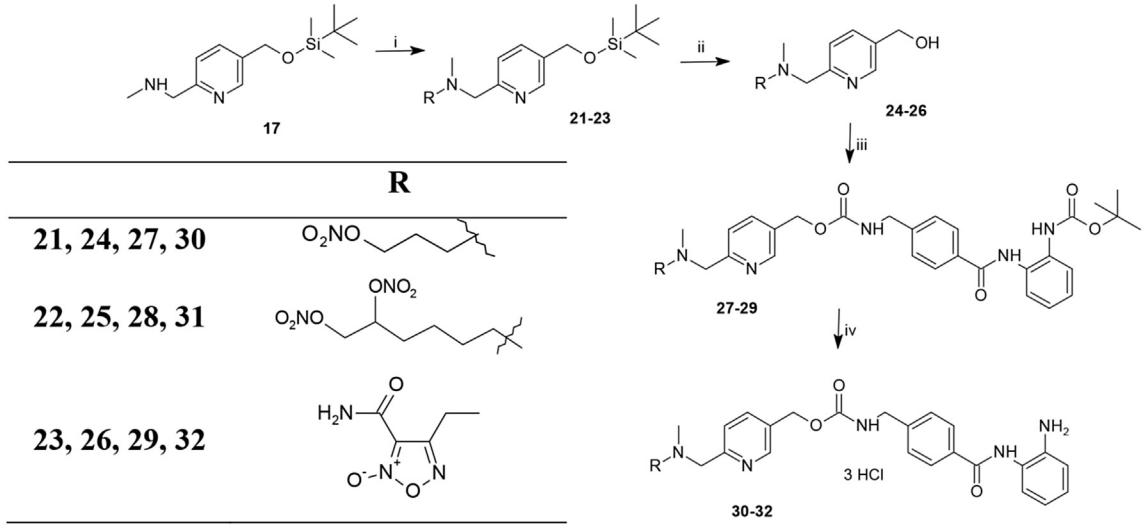

Scheme 2. Synthesis of compounds 30–32. Regents and conditions. i) $NaHCO_3$, acetone, **18** (3-bromopropylnitrate) or **19** (5,6-bisnitrooxyhexylmethanesulfonate) or **20** (4-bromomethylfuroxan-3-carboxamide); ii) $CH_3COOH/THF/H_2O$ (3/1/1 v/v/v), 4 days, r.t.; iii) CDI, **8**, dry THF; iv) 5.30 M HCl in 1,4-dioxane, THF.

compounds able to release NO only, as depicted in Scheme 3. The dinitrooxy derivative **33** was obtained by reaction of **19** with *N*,*N*-dimethylamine in EtOH, and was isolated as oxalate. Furoxan derivative **34** was obtained from the reaction of 3,4-bisphenylsulfonylfuroxan **12** and 2-methoxyethanol in CH_2Cl_2 using DBU as base.

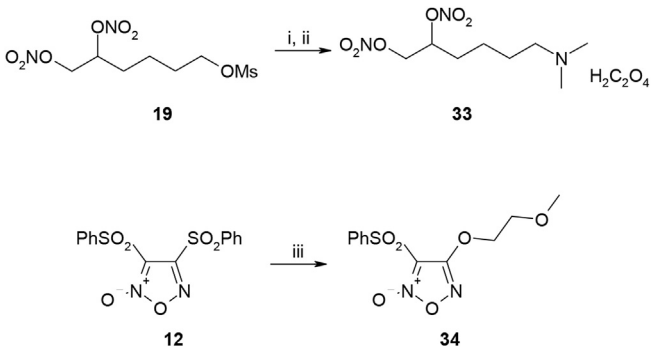

Scheme 3. Synthesis of compounds 33, 34. Regents and conditions. i) 5,6 M *N*,*N*-dimethylamine in EtOH, 50 °C; ii) $H_2C_2O_4$, EtOAc; iii) 2-methoxyethanol, DBU, CH_2Cl_2.

4. Biology

4.1. Single moiety activity preservation

Hybrid molecules were designed to avoid alteration of both the affinity for the active site of HDAC enzymes and the NO release ability. HDAC inhibition activity was preserved placing the linker on the most extremely variable part of the MS-275 pharmacophore

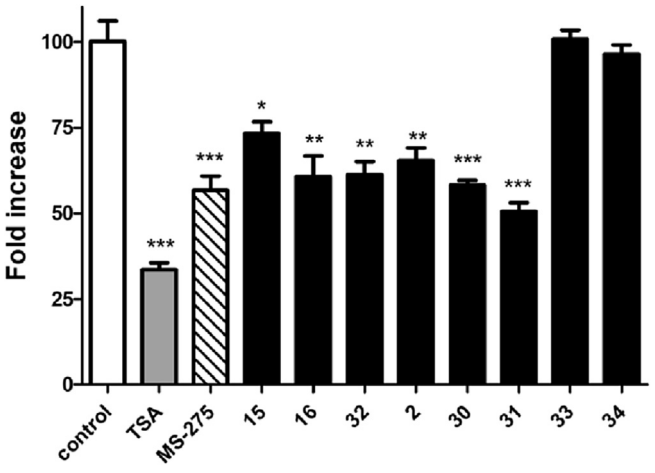

Fig. 2. Hybrids inhibition of total HDAC activity. Data are represented as means ± SEM; *p < .05; **p < .001; ***p < .0001; versus the control group (*t-test*).

(Fig. 1) and tested by HDAC activity assay. The assay was performed in HaCaT cell lysates after 1 h of treatment with 10 μM of MS-275, dinitrooxy (**33**) and phenylsulfonylfuroxan (**34**) compounds or with hybrids **15**, **16**, **32**, **30** and **31**. 100 nM of TSA, the most known potent HDACi,**[**7] and the previously studied hybrid **2 [**47] were used as control reference.

In vitro all hybrids significantly inhibited total HDAC activity determining a decrease from 20% to 50% compared to controls (Fig. 2). These results confirm previous prediction indicating that the conjugation of NO donor moieties does not significantly alter the affinity of the hybrid molecules to HDAC enzymes.

Moreover, since MS-275, a known class I HDAC selective inhibitor,**[**46] was used as building block for all our hybrid molecules, we evaluated the class I HDAC selective inhibitory activity also for compounds **16** and **31** (Fig. 3A–D*)* and their related IC_{50} values (Fig. 3E). The most characterized class I HDACs, HDAC1, HDAC2 and HDAC3, were overexpressed in recipient cells (Fig. 3A) and HDAC activity assay was performed (Fig. 3B, C and D).

Fig. 3 shows no relevant differences in term of HDAC inhibition in comparison to MS-275. Of note compounds **16** and **31** showed a lower IC_{50} value for HDAC2, an enzyme known to be inhibited also by *S*-nitrosylation [59].

The ability to release NO was evaluated in HaCaT cells by of 4,5-diaminofluorescein (DAF-2DA) fluorescence and FACS analysis after 1 h (Fig. 4A) to 5 h (Fig. 4B) of treatment with the synthetized hybrid molecules. As the balance is crucial in hybrid molecules, NO release was tested at the same concentration at which hybrid molecules displayed HDAC inhibition activity (10 μM). For this experiment, diethylenetriamine NONOate (DETA/NO), a spontaneous NO donor, and the previously characterized hybrid **2** [47] were used as positive controls. Results were consistent with the hybrid nature of the chemical structures (Fig. 4). Among nitrates, mononitrooxy compound **30** displayed hardly any ability to release

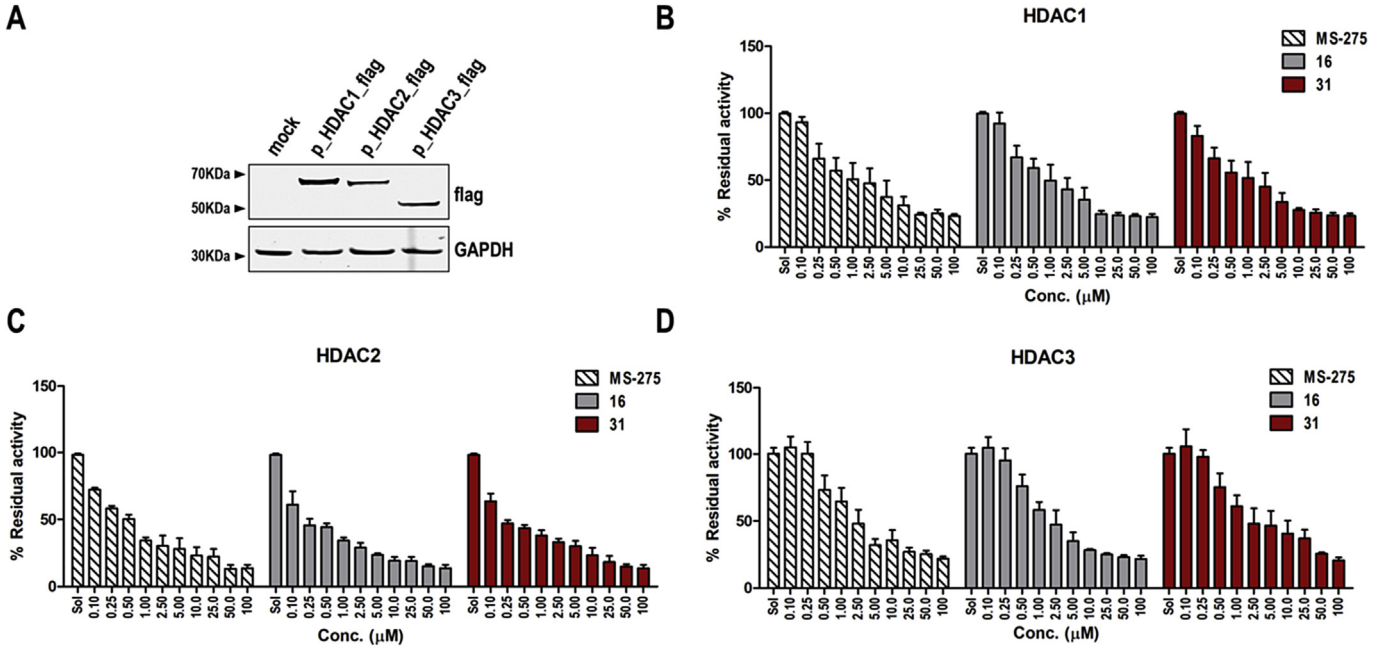

E

IC50 (μM)	MS-275	16	31
HDAC1	1,07 ± 0,53	1,02 ± 0,46	1,04 ± 0,50
HDAC2	0,74 ± 0,31	0,37 ± 0,14	0,39 ± 0,16
HDAC3	1,23 ± 0,49	1,19 ± 0,48	1,22 ± 0,49

Fig. 3. Class I HDAC selective inhibitory activity of compounds 16 and 31. (A) Representative western blot analysis of HDAC1, 2 and 3 expression in HEK293T cells after transfection. Signal was revealed by flag antibody and GAPDH was used as loading control. Three independent experiments were performed. **(B)** Compounds **16** and **31** inhibition of HDAC1 activity. MS-275 was used as control. Data are represented as means ± SEM. **(C)** Compounds **16** and **31** inhibition of HDAC2 activity. MS-275 was used as control. Data are represented as means ± SEM. **(D)** Compounds **16** and **31** inhibition of HDAC3 activity. MS-275 was used as control. Data are represented as means ± SEM. **(E)** IC_{50} values related to compounds **16** and **31** for HDAC1, 2 and 3.

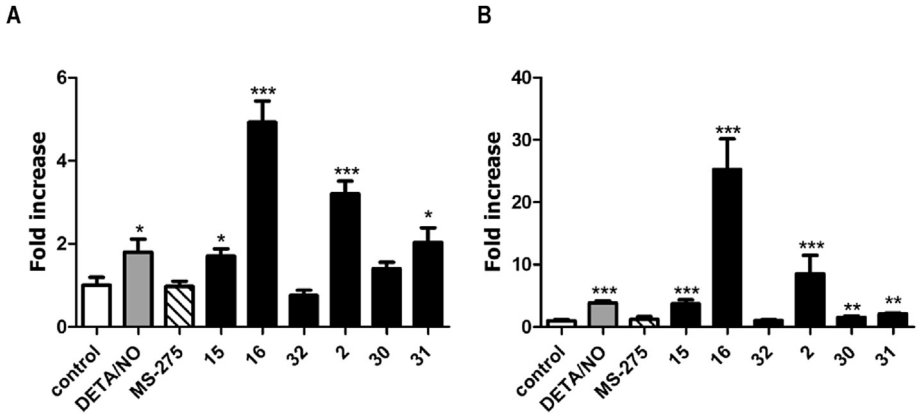

Fig. 4. Intracellular nitric oxide release of the designed hybrids. (A) Nitric oxide release evaluation after 1 h of treatment. **(B)** Nitric oxide release evaluation after 5 h of treatment. Data are represented as means ± SEM; *p < .05; **p < .001; ***p < .0001 versus control group (*t-test*).

NO at 10 μM, whereas, as expected, dinitrooxy compound **31**, at the same concentration, released more NO (Fig. 4). Among furoxans, compound **15**, bearing a phenylfuroxan moiety, displayed a weak NO donor ability, whereas compounds **16**, a phenylsulfonylfuroxan moiety, showed the highest NO release rate among furoxans and all the synthetized hybrids with a progressive time dependent increase (Fig. 4). Furoxancarboxyamide **32** did not release NO neither at 10 μM (Fig. 4) nor at 50 μM or 100 μM (data not shown). This behaviour was unexpected because furoxancarboxyamide moiety has been previously reported as a good NO donor-better than phenylfuroxan moiety-displaying vasodilating properties in rat aorta strips pre-contracted with phenylephrine [60]. At present, we cannot provide an explanation for this anomalous behaviour; further evaluations are required but they are not object of the present manuscript.

Taken together these results obtained from HDAC activity assay and DAF analysis showed pharmacologic potential for the synthetized molecules **16** and **31**. To further investigate the NO release ability, we performed some biochemical analysis to show their effect on both class I and class II HDACs. Indeed, NO directly induced class I HDAC2 *S*-nitrosylation [59,61] and class II HDAC4/5 shuttling into the nucleus with consequent histone deacetylation and gene repression [10,62]. *S*-nitrosylation of HDAC2, able to influence both the catalytic activity and the enzyme association to chromatin, has been tested in immunoprecipitation experiments after 1 h of HaCaT cells treatment with compounds **16** and **31**, the best NO donors according to FACS analysis (Fig. 5). In this experiment hybrid **2** [47] was used as positive control. All compounds were able to induce HDAC2 *S*-nitrosylation, suggesting that NO released from these hybrid molecules was able to chemically modify HDAC2 (Fig. 5). These data are in accordance with HDAC2 inhibitory activity observed in the presence of compounds **16** and **31** shown in Fig. 3C and E.

The NO-dependent translocation of class II HDACs was analysed by immunofluorescence on HaCaT cells treated for 1 h with 10 μM of compounds **16** and **31** (Fig. 6). As shown in Fig. 6, class II HDAC (HDAC4 and HDAC5) nuclear translocation was significantly promoted by treatments compared to control condition. This result suggests that the hybrids are still able to activate the nuclear shuttling mechanism of class II HDACs.

4.2. Vasodilating properties

The capacity of the hybrid NO-donor MS-275 analogues and of the reference compounds **33** and **34** to activate the soluble guanylyl cyclase (sGC) was evaluated through the ability of the products to induce vasodilation of rat aorta strips precontracted with phenylephrine, in the absence and in the presence of 1 μM ODQ (1*H*-1,2,4-oxadiazolo-4,3-a-quinoxalin-1-one), a well-known inhibitor of this enzyme. All the products were able to dilate the precontracted tissue in a concentration-dependent manner. The vasodilator potencies, expressed as EC_{50} values, are collected in Table 1. The most potent vasodilators were the phenylsulfonyl and the cyano substituted furoxan derivatives **16**, **34** and **2**, whose EC_{50} values fall in the sub-micromolar range. These products were about tenfold and one hundred fold more potent than the dinitrooxy substituted analogue **31** and **33** and the remaining compounds **15**, **30**, **32**, respectively. When the experiments were repeated in the presence of ODQ a marked decrease in the potencies was observed, so indicating the involvement of the sGC activation in the vasodilator action.

4.3. Functional analysis

Recently, we reported the ability of hybrid **2** to promote skeletal

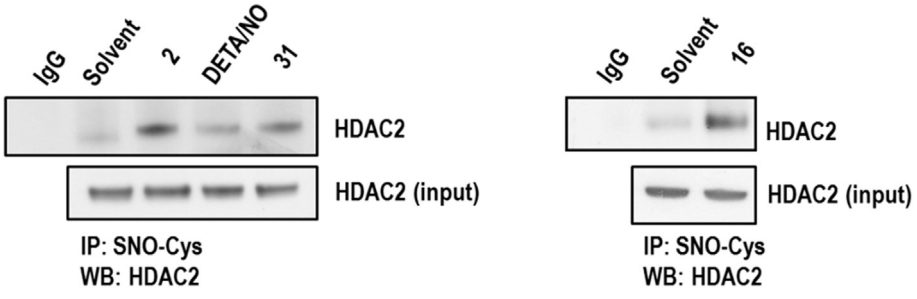

Fig. 5. Hybrid induction of HDAC2 *S*-nitrosylation. Representative immunoprecitation for *S*-nitrosocysteine revealed for HDAC2.

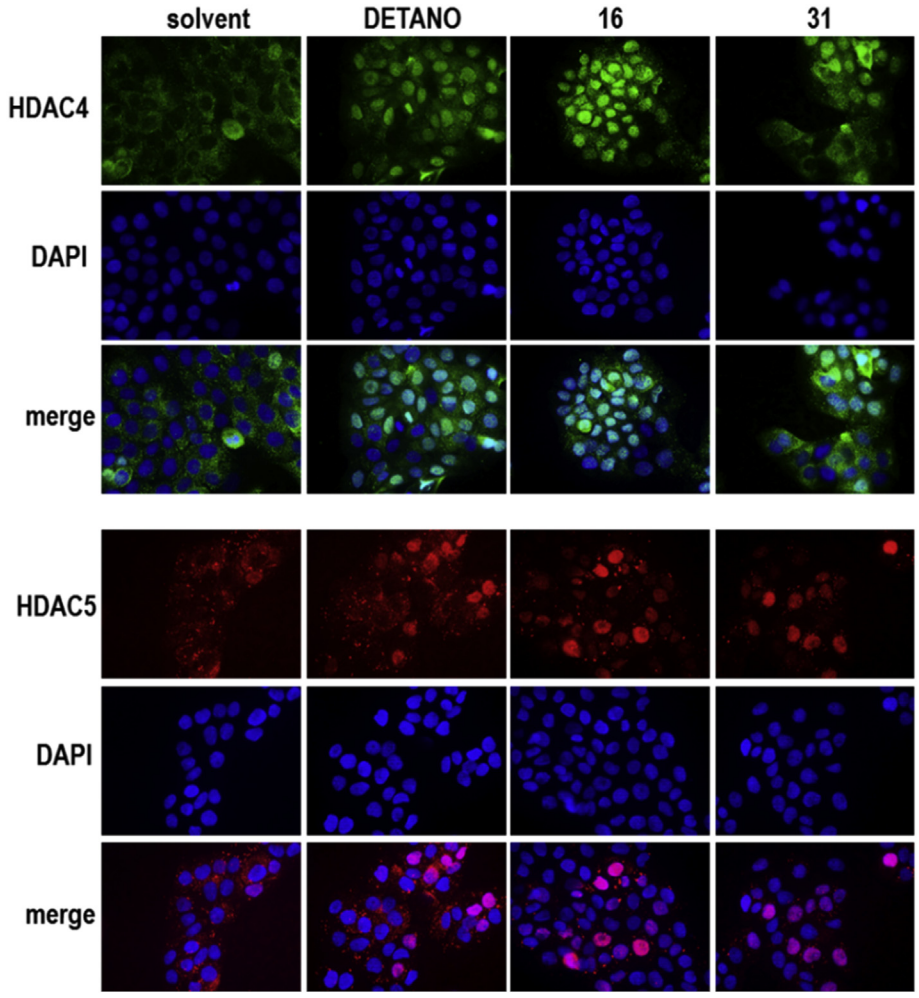

Fig. 6. Hybrid induction of class II HDAC shuttling from cell cytoplasm to the nucleus. Representative immunofluorescence panels revealed for HDAC4 (green) and HDAC5 (red). Nuclei counterstained with DAPI (blue). Magnification 40×.

muscle differentiation promoting formation of large fused myotubes with a high nuclei/fibre ratio [47]. This effect was significantly higher than that obtained by the single hybrid components possibly in consequence of the combined effect of NO on class II HDACs, the nitrosylation of HDAC2 and the overall inhibition of class I HDAC activity [47]. According to the experimental evidences, the newly synthetized hybrid molecules **16** and **31** were the most promising compounds for skeletal muscle differentiation. C2C12 cells, a mouse myoblast cell line, were cultured in 20% serum (growth medium; GM) until differentiation induction by serum lowering to 2% (differentiation medium; DM). Differentiation was stimulated in the presence of 0.5 μM hybrid compounds **16** or **31**. Control cells were differentiated in the presence of separated or combined pharmacophores (phenylsulfonylfuroxan - **34** - and MS-275 for compound **16** and dinitrooxy - **33** - and MS-275 for compound **31**) (Fig. 7). After 5 days, differentiation response was evaluated by myosin heavy chain (MHC) expression (Fig. 7A), by evaluation of nuclei/fiber ratio (Fig. 7B) and by a panel of muscle differentiation markers, such as myomaker (MyoM), myogenin (MyoG) and myogenic regulatory factor 4 (MRF4) (Fig. 7C). Fig. 7 panel A shows that **31** promotes formation of larger myotubes in comparison to **16.** The evaluation of the number of nuclei per fiber points out that compound **31** induces more multinucleated fibers than the combined pharmacophores (Fig. 7B). The ability of **31** to stimulate fusion among myoblasts is further confirmed by the high expression of MyoM, the membrane activator of myoblast fusion [63], depicted in Fig. 7, panel C.

Table 1
Vasodilator activity of the designed hybrids.

Compound	Vasodilator activity	
	EC_{50} (μM) ± SE	EC_{50} (μM) ± SE + ODQ 1 μM
15	3.4 ± 0.5	>100
16	0.031 ± 0.004	0.35 ± 0.08
30	2.6 ± 0.8	44 ± 1
31	0.29 ± 0.07	11 ± 3
32	3.4 ± 0.6	63 ± 12
33	0.80 ± 0.20	˃ 100
34	0.0045 ± 0.0001	0.43 ± 0.02
2	0.024 ± 0.005	0.96 ± 0.20

As demonstrated compounds **16** and **31** showed an interesting therapeutic potential. For this reason we tested their cytotoxic effect on HaCaT and C2C12 cells. Fig. 8A and B showed that both hybrid molecules were less toxic than MS-275 and compound 31 confirmed to be the most promising hybrids among the molecules here tested.

5. Conclusions

These data describe a group of novel hybrid compounds where

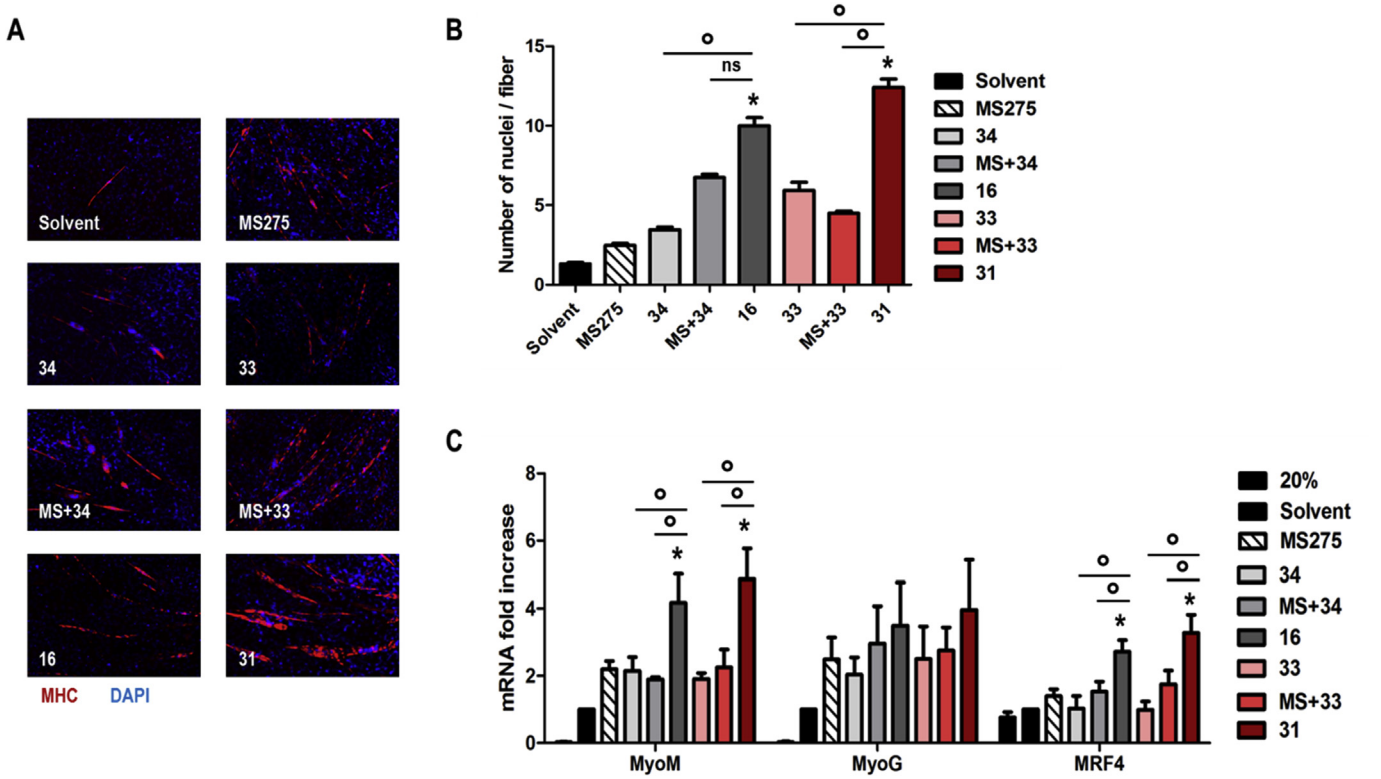

Fig. 7. Hybrid induction of skeletal muscle differentiation. (A) Representative immunofluorescence panels revealed for MHC (red). Nuclei counterstained with DAPI (blue). Magnification 20×. **(B)** Number of nuclei per myofiber quantification in C2C12 after 5 days of differentiation in the presence of 0.5 μM hybrid. Data are represented as means ± SEM; *p < .05 versus MS-275 group (*t-test*); °p < .05 (*t-test*). **(C)** Myomaker (MyoM), myogenin (MyoG) and myogenic regulatory factor 4 (MRF4) mRNA expression in C2C12 after 5 days of differentiation in the presence of 0.5 μM hybrid. Data are represented as fold increase in comparison to solvent condition group. Data are represented as means ± SEM; *p < .05 versus MS-275 group (*t-test*); °p < .05 (*t-test*).

various NO-donor groups (phenylsulfonylfuroxan, dinitrooxy) are coupled with the class I HDAC inhibitor MS-275. Interestingly, these hybrids distinctly affect HDAC activity inhibiting class I by MS-275- and NO-dependent (*S*-nitrosylation) effect and activating class II via NO-dependent cytosol-nuclear shuttling. Functionally, this family of compounds exhibit specific and unique biological features to control muscle differentiation and *ex vivo* aortic vasodilatation. Overall we identified novel promising compounds that may be apply in different pathological context such as cardiovascular, neuromuscular and inflammatory disorders.

6. Author contribution

SA carried out experiments and data analysis; KC carried out the synthesis; CC carried out experiments and data analysis and wrote the manuscript; SG carried out the synthesis, EM carried out

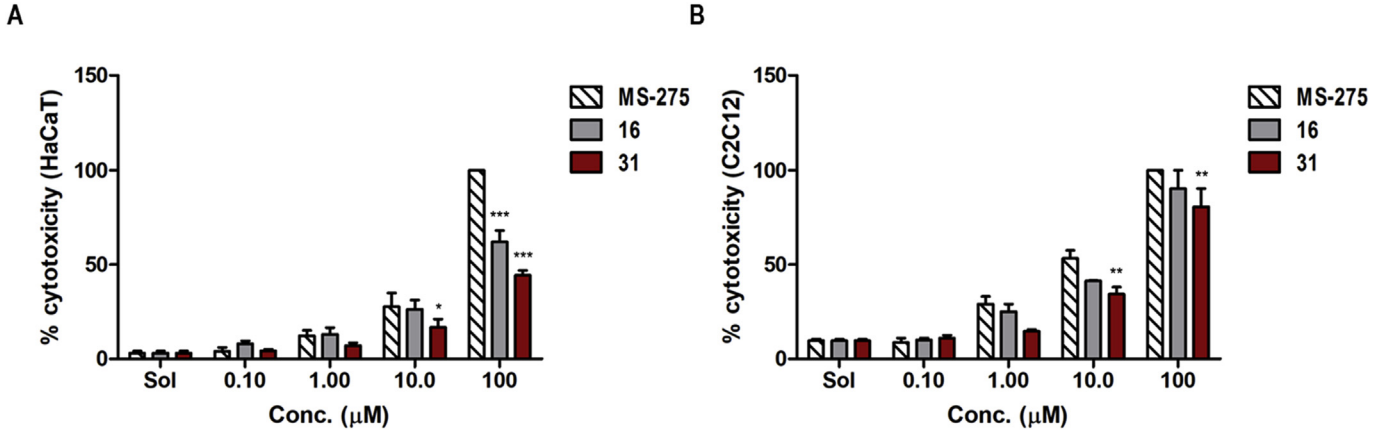

Fig. 8. Cytotoxicity evaluation of compounds 16 and 31. (A) Percentage of cytotoxicity in HaCaT cells expressed as percentage of death cells in response to different concentrations of compound **16** and **31** compared to MS-275. Data are represented as means ± SEM; *p < .05; ***p < .001 versus MS-275 group (ANOVA test). **(B)** Percentage of cytotoxicity in C2C12 cells expressed as percentage of death cells in response to different concentrations of compound **16** and **31** compared to MS-275. Data are represented as means ± SEM; **p < .01 versus MS-275 group (ANOVA test).

experiments and data analysis, CG revised data analysis and the manuscript; RF revised the manuscript; FS conceived and carried out the experiments and wrote the manuscript; LL conceived and carried out the synthesis and wrote the manuscript. All the authors contributed critical discussion and approved the final version of the manuscript.

Acknowledgements

The authors wish to thank Prof. Alberto Gasco (Università degli Studi di Torino).

The present study was supported by LOEWE Cell & Gene Therapy Center (LOEWE-CGT) Goethe University Frankfurt to CG and by Deutsche Forschungsgemeinschaft Program SFB834 "Endothelial Signaling and Vascular Repair," project B11 to CG. FS is the recipient of the LOEWE CGT grant # III L 5 - 518/17.004 (2013) and funded by the DFG (German Research Foundation), "Excellence Cluster Cardio Pulmonary System." CC is the recipient of the Start-up grant 2016 from LOEWE-Forschungszentrum für Zell-und Gentherapie, gefördert durch das Hessische Ministerium für Wissenschaft und Kunst. Aktenzeichen: III L 5 - 491 518/17.004 (2013).

The present study was supported by the University of Turin (Ricerca Locale ex 60%).

Appendix A. Supplementary data

Supplementary data related to this article can be found at https://doi.org/10.1016/j.ejmech.2017.12.047.

References

[1] X.J. Yang, E. Seto, Lysine acetylation: codified crosstalk with other post-translational modifications, Mol. Cell. 31 (2008) 449–461.
[2] C. Hildmann, D. Riester, A. Schwienhorst, Histone deacetylases - an important class of cellular regulators with a variety of functions, Appl. Microbiol. Biotechnol. 75 (2007) 487–497.
[3] B. Illi, C. Colussi, A. Grasselli, A. Farsetti, M.C. Capogrossi, C. Gaetano, NO sparks off chromatin: tales of a multifaceted epigenetic regulator, Pharmacol. Ther 123 (2009) 344–352.
[4] A. Mai, S. Massa, D. Rotili, I. Cerbara, S. Valente, R. Pezzi, S. Simeoni, R. Ragna, Histone deacetylation in epigenetics: an attractive target for anticancer therapy, Med. Res. Rev. 25 (2005) 261–309.
[5] U.H. Weidle, A. Grossmann, Inhibition of histone deacetylases: a new strategy to target epigenetic modifications for anticancer treatment, Anticancer Res. 20 (2000) 1471–1485.
[6] P. Bertrand, Inside HDAC with HDAC inhibitors, Eur. J. Med. Chem. 45 (2010) 2095–2116.
[7] M. Yoshida, M. Kijima, M. Akita, T. Beppu, Potent and specific inhibition of mammalian histone deacetylase both in vivo and in vitro by trichostatin A, J. Biol. Chem. 265 (1990) 17174–17179.
[8] M. Duvic, R. Talpur, X. Ni, C. Zhang, P. Hazarika, C. Kelly, J.H. Chiao, J.F. Reilly, J.L. Ricker, V.M. Richon, S.R. Frankel, Phase 2 trial of oral vorinostat (suberoylanilide hydroxamic acid, SAHA) for refractory cutaneous T-cell lymphoma (CTCL), Blood 109 (2007) 31–39.
[9] C. Zagni, G. Floresta, G. Monciino, A. Rescifina, The search for potent, small-molecule HDACis in cancer treatment: a decade after vorinostat, Med. Res. Rev. 37 (6) (2017) 1373–1428.
[10] B. Illi, C.D. Russo, C. Colussi, J. Rosati, M. Pallaoro, F. Spallotta, D. Rotili, S. Valente, G. Ragone, F. Martelli, P. Biglioli, C. Steinkuhler, P. Gallinari, A. Mai, M.C. Capogrossi, C. Gaetano, Nitric oxide modulates chromatin folding in human endothelial cells via protein phosphatase 2A activation and class II histone deacetylases nuclear shuttling, Circ. Res. 102 (2008) 51–58.
[11] G. Blander, L. Guarente, The Sir2 family of protein deactylases, Annu. Rev. Biochem. 73 (2004) 417–435.
[12] K. Chen, L. Xu, O. Wiest, J. Org. Chem. 78 (2013) 5051–5055.
[13] A.M. Grabiec, S. Krausz, W. De Jager, T. Burakowski, D. Groot, M.E. Sanders, B.J. Prakken, W. Maslinski, E. Eldering, P.P. Tak, K.A. Ridquist, Histone deacetylase inhibitors suppress inflammatory activation of rheumatoid arthritis patient synovial macrophages and tissue, J. Immunol. 184 (2010) 2718–2728.
[14] C. Colussi, B. Illi, J. Rosati, F. Spallotta, A. Farsetti, A. Grasselli, A. Mai, M.C. Capogrossi, C. Gaetano, Histone deacetylase inhibitors: keeping momentum for neuromuscular and cardiovascular diseases treatment, Pharmacol. Res. 62 (2010) 3–10.
[15] G.C. Minetti, C. Colussi, R. Adami, C. Serra, C. Mozzetta, V. Parente, S. Fortuni, S. Straino, M. Sampaolesi, M. Di Padova, B. Illi, P. Gallinari, C. Steinkuhler, M.C. Capogrossi, V. SArtorelli, R. Bottinelli, C. Gaetano, P.L. Puri, Functional and morphological recovery of dystrophic muscles in mice treated with deacetylase inhibitors, Nat. Med. 12 (2006) 1147–1150.
[16] F. Coppedè, The potential of epigenetic therapies in neurodegenerative diseases, Front. Genet. 5 (2014), 220.
[17] S. Consalvi, C. Mozzetta, Preclinical studies in the mdx mouse model of duchenne muscular dystrophy with the histone deacetylase inhibitor, Givinostat. Mol. Med 19 (2013) 79–87.
[18] P. Bettica, S. Petrini, V. D'Oria, A. D'Amico, M. Catteruccia, M. Pane, S. Sivo, F. Magri, S. Brajkovic, S. Messina, G.L. Vita, B. Gatti, M. Moggio, P.L. Puri, M. Rocchetti, G. De Nicolao, G. Vita, G.P. Comi, E. Bertini, E. Mercuri, Histological effects of givinostat in boys with Duchenne muscular dystrophy, Neuromuscul. Disord. 26 (2016) 643–649.
[19] H. Dabiré, I. Barthlemy, N. Blanchard-Gutton, L. Sambin, C.C. Sampedrano, V. Gouni, Y. Unterfinger, P. Aguilar, J.-L. Thibaud, B. Ghaleh, A. Bizet, G.-L.-Pouchelon, S. Blot, A. Berdeaux, L. Ittinger, V. Chetboul, J.B. Su, Vascular endothelial dysfunction in Duchenne muscular dystrophy is restored by bradykinin through upregulation of eNOS and nNOS, Basic Res. Cardiol. 107 (2012), 240.
[20] R.C. Jin, J. Loscalzo, Vascular nitric oxide: formation and function, J. Blood Med 1 (2010) 147–162.
[21] D. Tousoulis, A.-M. Kampoli, C. Tentolouris, N. Papageorgiou, C. Stefanadis, The role of nitric oxide on endothelial function, Curr. Vasc. Pharmacol. 10 (2012) 4–18.
[22] J.E. Albina, J.S. Reichner, Role of nitric oxide in mediation of macrophage cytotoxicity and apoptosis, Canc. Metastasis Rev. 17 (1998) 39–53.
[23] C. Bogdan, Nitric oxide and the immune response, Nat. Immunol. 2 (2001) 907–916.
[24] D. Hirst, T. Robson, Targeting nitric oxide for cancer therapy, J. Pharm. Pharmacol. 59 (2007) 3–13.
[25] J.L. Wallace, Nitric oxide as a regulator of inflammatory processes, Mem. Inst. Oswaldo Cruz 100 (2005) 5–9.
[26] B.-M. Choi, H.-O. Pae, S. Jang, Y.-M. Kim, H.-T. Chung, Nitric oxide as a pro-apoptotic as well as anti-apoptotic modulator, J. Biochem. Mol. Biol. 35 (2002) 116–126.
[27] M. Lepoivre, J.M. Flaman, Y. Henry, Early loss of the tyrosyl radical in ribonucleotide reductase of adenocarcinoma cells producing nitric oxide, J. Biol. Chem. 267 (1992) 22994–23000.
[28] S. Baritaki, S. Huerta-Yepez, A. Sahakyan, I. Karagiannides, K. Bakirtzi, A.R. Jazirehi, B. Bonavida, J.F. Kugel, Mechanisms of nitric oxide-mediated inhibition of EMT in cancer: inhibition of the metastasis-inducer snail and induction of the metastasis-suppressor RKIP, Cell Cycle 9 (2010) 4931–4940.
[29] B. Bonavida, S. Baritaki, Inhibition of epithelial-to-mesenchymal transition (EMT) in cancer by nitric oxide: pivotal roles of nitrosylation of NF-κB, YY1 and snail, Forum Immunopathol. Dis. Ther. 3 (2012) 125–133.
[30] B. Bonavida, S. Baritaki, S. Huerta-Yepez, M.I. Vega, D. Chatterjee, K. Yeung, Novel therapeutic applications of nitric oxide donors in cancer: roles in chemo- and immunosensitization to apoptosis and inhibition of metastases, Nitric Oxide - Biol. Chem. 19 (2008) 152–157.
[31] H. Yasuda, M. Yamaya, K. Nakayama, T. Sasaki, S. Ebihara, A. Kanda, M. Asada, D. Inoue, T. Suzuki, T. Okazaki, H. Takahashi, M. Yoshida, T. Kaneta, K. Ishizawa, S. Yamanda, N. Tomita, M. Yamasaki, A. Kikuchi, H. Kubo, H. Sasaki, Randomized phase II trial comparing nitroglycerin plus vinorelbine and cisplatin with vinorelbine and cisplatin alone in previously untreated stage IIIB/IV non-small-cell lung cancer, J. Clin. Oncol. 24 (2006) 688–694.
[32] H. Yasuda, K. Nakayama, M. Watanabe, S. Suziki, H. Fuji, S. Okinaga, A. Kanda, K. Zaiasu, T. Sasaki, M. Asada, T. Suzuki, M. Yoshida, S. Yamanda, D. Inoue, T. Kaneta, T. Kondo, Y. Takai, H. Sasaki, K. Yanagiara, M. Yamaya, Nitroglycerin treatment may enhance chemosensitivity to docetaxel and carboplatin in patients with lung adenocarcinoma, Clin. Canc. Res. 12 (2006) 6748–6757.
[33] B. Bonavida, S. Baritaki, Dual role of NO donors in the reversal of tumor cell resistance and EMT: downregulation of the NF-κB/Snail/YY1/RKIP circuitry, Nitric Oxide - Biol. Chem. 24 (2011) 1–7.
[34] D.H. Lee, G.P. Pfeifer, Mutagenesis induced by the nitric oxide donor sodium nitroprusside in mouse cells, Mutagenesis 22 (2007) 63–67.
[35] J.V. Esplugues, NO as a signalling molecule in the nervous system, Br. J. Pharmacol. 135 (2002) 1079–1095.
[36] J.S. Stamler, G. Meissner, Physiology of nitric oxide in skeletal muscle, Physiol. Rev. 81 (2001) 209–237.
[37] J.E. Anderson, A Role for nitric oxide in muscle repair : nitric oxide – mediated activation of muscle satellite cells, Mol. Biol. Cell 11 (2000) 1859–1874.
[38] J.L. Betters, V.A. Lira, Q.A. Soltow, J.A. Drenning, D.S. Criswell, Supplemental nitric oxide augments satellite cell activity on cultured myofibers from aged mice, Exp. Gerontol. 43 (2008) 1094–1101.
[39] L.I. Filippin, A.J. Moreira, N.P. Marroni, R.M. Xavier, Nitric oxide and repair of skeletal muscle injury, Nitric Oxide 21 (2009) 157–163.
[40] S. Brunelli, C. Sciorati, G. D'Antona, A. Innocenzi, D. Covarello, B.G. Galvez, C. Perrotta, A. Monopoli, F. Sanvito, R. Bottinelli, E. Ongini, G. Cossu, E. Clementi, Nitric oxide release combined with nonsteroidal antiinflammatory activity prevents muscular dystrophy pathology and enhances stem cell therapy, Proc. Natl. Acad. Sci. U. S. A 104 (2007) 264–269.
[41] C. Colussi, A. Gurtner, J. Rosati, B. Illi, G. Ragone, G. Piaggio, M. Moggio, C. Lamperti, G. D'Angelo, E. Clementi, G. Minetti, C. Mozzetta, A. Antonini, M.C. Capogrossi, P.L. Puri, C. Gaetano, Nitric oxide deficiency determines global chromatin changes in Duchenne muscular dystrophy, Faseb. J. 23

(2009) 2131–2141.
[42] C. Sciorati, B.G. Galvez, S. Brunelli, E. Tagliafico, S. Ferrari, G. Cossu, E. Clementi, Ex vivo treatment with nitric oxide increases mesoangioblast therapeutic efficacy in muscular dystrophy, J. Cell Sci. 119 (2006) 5114–5123.
[43] V. Voisin, C. Sebrièe, S. Matecki, H. Yu, B. Gillet, M. Ramonatxo, M. Israel, S. De La Porte, L-arginine improves dystrophic phenotype in mdx mice, Neurobiol. Dis. 20 (2005) 123–130.
[44] K.R. Wagner, Approaching a new age in Duchenne muscular dystrophy treatment, Neurotherapeutics 5 (2008) 583–591.
[45] C. Colussi, R. Berni, G. Rosati, S. Straino, S. Vitale, F. Spallotta, S. Baruffi, L. Bocchi, F. Delucchi, S. Rossi, M. Savi, D. Rotili, F. Quaini, E. MacChi, D. Stilli, E. Musso, A. Mai, C. Gaetano, M.C. Capogrossi, The histone deacetylase inhibitor suberoylanilide hydroxamic acid reduces cardiac arrhythmias in dystrophic mice, Cardiovasc. Res. 87 (2010) 73–82.
[46] A. Saito, T. Yamashita, Y. Mariko, Y. Nosaka, K. Tsuchiya, T. Ando, T. Suzuki, T. Tsuruo, O. Nakanishi, A synthetic inhibitor of histone deacetylase, MS-27-275, with marked in vivo antitumor activity against human tumors, Proc. Natl. Acad. Sci. U. S. A 96 (1999) 4592–4597.
[47] E. Borretto, L. Lazzarato, F. Spallotta, C. Cencioni, Y. D'alessandra, C. Gaetano, R. Fruttero, A. Gasco, Synthesis and biological evaluation of the first example of NO-donor histone deacetylase inhibitor, ACS Med. Chem. Lett. 4 (2013) 994–999.
[48] A. Daiber, P. Wenzel, M. Oelze, T. Münzel, New insights into bioactivation of organic nitrates, nitrate tolerance and cross-tolerance, Clin. Res. Cardiol. 97 (2008) 12–20.
[49] A. Gasco, K. Schoenafinger, in: P.G. Wang, T.B. Cai, N. Taniguchi (Eds.), Nitric Oxide Donors, Verlag GmbH & Co KGaA Weinheim, 2005, pp. 131–175.
[50] R. Blunt, A.J: Eatherton, V. Garzya, M.P. Healy, J. Myatt, R.A. Porter, Benzoxazinone Derivatives for the Treatment of Glytimediated Disorders. WO2011/012622A1.
[51] P.G. McDougal, J.G. Rico, Y.I. Oh, B.D. Condon, A convenient procedure for the monosilylation of symmetric 1,n-diols, J. Org. Chem. 51 (1986) 3388–3390.
[52] D. Schuppan, C. Herold, M. Gansmayer, M. Ocker, New Pharmaceutical Combination, WO2004/058234, July 15, 2004.
[53] G. Sorba, G. Ermondi, R. Fruttero, U. Galli, A. Gasco, Unsymmetrically substituted furoxans. XVI. Reaction of benzenesulfonyl substituted furoxans with ethanol and ethanethiol in basic medium, J. Heterocycl. Chem. 33 (1996) 327–334.
[54] R. Shan, C. Velazquez, E. Knaus, Syntheses, calcium channel agonist-antagonist modulation activities, and nitric oxide release studies of nitrooxyalkyl 1,4-dihydro-2,6-dimethyl-3-nitro-4-(2,1,3-benzoxadiazol-4-yl)pyridine-5-carboxylate racemates, enantiomers, and diastereomers, J. Med. Chem. 47 (2004) 254–261.
[55] A. Di Stilo, S. Visentin, C. Cena, A.M. Gasco, G. Ermondi, A. Gasco, New 1,4-dihydropyridines conjugated to furoxanyl moieties, endowed with both nitric oxide-like and calcium channel antagonist vasodilator activities, J. Med. Chem. 41 (1998) 5393–5401.
[56] C. Cena, K. Chegaev, S. Balbo, L. Lazzarato, B. Rolando, M. Giorgis, E. Marini, R. Fruttero, A. Gasco, Novel antioxidant agents deriving from molecular combination of vitamin C and NO-donor moieties, Bioorg. Med. Chem. 16 (2008) 5199–5206.
[57] M. Bertinaria, P. Orjuela-Sanchez, E. Marini, S. Guglielmo, A. Hofer, Y.C. Martins, G.M. Zanini, J.A. Frangos, A. Gasco, R. Fruttero, L.J.M. Carvalho, O-donor dihydroartemisinin derivatives as multitarget agents for the treatment of cerebral malaria, J. Med. Chem. 58 (2015) 7895–7899.
[58] S. Emiliani, W. Fischle, C. Van Lint, Y. Al-Abed, E. Verdin, Characterization of a human RPD3 ortholog, HDAC3, Proc Natl Acad Sci U S A 95 (6) (1998) 2795–2800.
[59] C. Colussi, C. Mozzetta, A. Gurtner, B. Illi, J. Rosati, S. Straino, G. Ragone, M. Pescatori, G. Zaccagnini, A. Antonini, G. Minetti, F. MArtelli, G. Piaggio, P. Gallinari, C. Steinkulher, E. Clementi, C. Dell'Aversana, L. Altucci, A. Mai, M.C. Capogrossi, P.L. Puri, C. Gaetano, HDAC2 blockade by nitric oxide and histone deacetylase inhibitors reveals a common target in Duchenne muscular dystrophy treatment, Proc. Natl. Acad. Sci. U. S. A 105 (49) (2008) 19183–19187.
[60] R. Fruttero, D. Boschi, A. Di Stilo, A. Gasco, The furoxan system as a useful tool for balancing 'hybrids' with mixed alfa1-antagonist and NO-like vasodilator activities, J. Med. Chem. 38 (1995) 4944–4949.
[61] A. Nott, P.M. Watson, J.D. Robinson, L. Crepaldi, A.S. Riccio, Nitrosylation of histone deacetylase 2 induces chromatin remodelling in neurons, Nature 455 (2008) 411–415.
[62] F. Spallotta, J. Rosati, S. Straino, S. Nanni, A. Grasselli, V. Ambrosino, D. Rotili, S. Valente, A. Farsetti, A. Mai, M.C. Capogrossi, C. Gaetano, B. Illi, Nitric oxide determines mesodermic differentiation of mouse embryonic stem cells by activating class IIa histone deacetylases: potential therapeutic implications in a mouse model of hindlimb ischemia, Stem Cells. 28 (2010) 431–442.
[63] D.P. Millay, J.R. O'Rourke, L.B. Sutherland, S. Bezprosvannaya, J.M. Shelton, R. Bassell-Dubay, E.M. Olson, Myomaker is a membrane activator of myoblast fusion and muscle formation, Nature 499 (2013) 301–305.